Modelling differential geomorphic effectiveness in neighbouring upland catchments: implications for sediment and flood risk management in a wetter world

David J. Milan

Department of Geography, Geology and Environment, University of Hull, UK

d.milan@hull.ac.uk

KEYWORDS:, sensitivity, threshold, recovery, connectivity, resilience

Abstract

In July 2007 an intense summer storm resulted in significant activation of the sediment system in the Thinhope Burn, UK. Catchment- and reach-scale morphodynamic modelling is used to investigate the geomorphic work undertaken by Thinhope Burn; comparing this with the more subdued responses shown by its neighbours. Total sediment efflux for Thinhope Burn over the 10 yr period 1998-2008 was 18801 m^3 four times that of the larger Knar catchment and fifty-four times that of the smaller Glendue Burn catchment. For a discharge of 60 m^3s^{-1}, equivalent to the July 2007 Thinhope flood, sediment efflux was 575 m^3, 76 m^3, and 67 m^3 for Thinhope, Glendue and Knar Burns respectively. It is clear that Thinhope Burn undertook significantly more geomorphic work compared to its neighbours. Analysis of the population of shear stress for reach-scale simulations on Thinhope Burn highlighted that the final three simulations (flood peaks of 60, 90, 236 m^3s^{-1}) all produced very similar distributions, with no marked increase in the modal shear stress (~250 Nm^{-2}). This possibly suggests that flows >60 m^3s^{-1} are not able to exert significantly greater energy on the channel boundary, indicating that flows in the region of 60 m^3s^{-1} attain 'peak' geomorphic work. It is argued that factors such as strength resistance of the key sediment sources (e.g. paleoberms perched on terraces), structural resistance to flood waves imposed by valley form resistance, location sensitivity and transmission resistance, may all offer explanations for increased geomorphic effectiveness compared with its neighbours. With the expectation of greater rainfall totals in the winter and more extreme summer events in upland areas of the UK, it is clear that attention needs to focus upon the implications of this upon the morphological stability of these areas not least to aid future sustainable flood risk management.

Introduction

Globally, there has been increased recent interest in flash flooding in low latitudes (Wohl et al., 2012; Quesada-Román et al., 2020a,b), upland and mountain river systems due to the uncertainty imposed by climate change (Gaume et al., 2015; Modrick and Georgakakos, 2015; Stoffel et al., 2016). Upland areas are particularly susceptible to flash flooding, which is one of the top-ranked causes of fatalities among natural disasters globally (Borga et al., 2011; Hopkins and Warburton, 2018). Increased heavy precipitation at regional (Groisman et al., 2004) and global scales (Groisman et al., 2005; Beniston, 2009) is thought to be linked with global warming (Huntington, 2006; Kenden et al., 2014; Wilby et al., 2018; Otto et al., 2018), and consequently the hazard imposed by flash flooding is expected to increase in frequency and severity (Kleinen and Petschel-Held, 2007; Beniston et al., 2011). Over the last 15 years in the UK, and co-incident with the current wet-phase in UK climate (Wilby et al., 2008; Dadson et al., 2017), there have been a number of events that have activated upland sediment systems, causing problems to bridge infrastructure and flooding, notably including the Storm Desmond impacts on upland streams in the Lake District (Joyce et al., 2018; Heritage et al., 2019). Flooding in upland areas also has economic impacts, and in the UK, damage caused by fluvial flooding is estimated to cost its economy ~£1.1 billion annually (Sayers et al., 2020).

Upland geomorphic response to extreme events

In the UK uplands, occasional extreme rainfall events can trigger a dramatic geomorphic response, whereby the full sediment system may be activated; resulting in active slope supply to river channels (Harvey, 1986; Harvey, 2007), and significant channel bed and floodplain mobilisation (Newson, 1980; Carling, 1986; Warburton, 2010; Milan, 2012; Joyce et al., 2018). Such events may be considered unusual in a number of respects. For example peat 'slides' or 'bog-bursts', caused by high soil water pressures, and often lubricated by water accumulating at the interface between peat and underlying till or bedrock, can supply large volumes of organic-rich sediment to first and second order streams (Newson, 1980; Carling, 1986; Large, 1991; Dykes and Warburton, 2007). Slopes that are connected to the channel in first and second order tributaries can supply enough sediment to change channel morphology a short distance downstream (Harvey 2001). Large boulders, in some cases metre-size, can be transported (Carling, 1983, Milan, 2012), and bedload transport rates can be very high sometimes aided by non-Newtonian sediment transport processes (e.g. Rickenmann, 1991), and accompanied by channel morphological change (*sensu* Brierley and Fryirs, 2016): such as channel widening and a switch from single- to multithread (Harvey, 2001; Milan, 2012). Very few studies have fully quantified the morphological response of river channels following such 'state-change' events (Graf, 1979; Knox, 1993; Phillips, 2014; Brierley and Fryirs, 2016), nor the recovery in the years following the event (Fryirs, 2017). Furthermore, there has been limited work investigating the factors responsible for sporadic incidences of enhanced catchment-scale 'effectiveness' (*sensu* Lisenby et al., 2018) to high magnitude events; whereby extreme volumes of bedload are transported (geomorphic work) over relatively short time periods at a centennial timescale.

Improved strategies for the management of sediment transfer in upland areas may be necessary for improved flood risk management in the future, which will need to be informed by an improved understanding of the geomorphic response of catchments to extreme events, and identification of those catchments that are likely to respond to extrinsic threshold exceedance related to increased flow magnitude and frequency driven by climate change. However, the relationship between cause (floods) and effect (sediment system and channel response) is acknowledged to be complex and non-linear (Phillips, 1992). There is a need for future sediment management for flood risk in upland areas to consider the concept of 'geomorphic effectiveness' (Lisenby et al., 2018), in parallel with a suite of other interrelated, fundamental geomorphic concepts (Table 1) including: landscape 'sensitivity' (Brunsden and Thornes, 1979; Fryirs, 2017), extrinsic/intrinsic 'thresholds' (Schumm, 1979; Beven, 1981), 'connectivity' (Fryirs, 2013; Bracken et al., 2015; Heckman et al., 2018), 'recovery' (Harvey, 2007; Fryirs and Brierley, 2000), and 'event sequencing' (Beven, 1981).

Table 1 Defining fundamental geomorphic concepts.

This paper uses morphodynamic modelling to investigate the differential geomorphic response of three small neighbouring catchments to different magnitude flood events; and discusses the results in the context of these geomorphic concepts, and associated implications for upland flood risk and sediment management. Specifically, the paper aims to:

1) Explore differential catchment- and reach-scale effectiveness through simulating geomorphic work;

2) Identify catchment- and reach-scale threshold exceedance for sediment stores.

Study Location and Hydrological Event

The study focused upon three neighbouring tributary catchments to the River South Tyne, Cumbria, UK: Knar Burn, Thinhope Burn and Glendue Burn (Figure 1, 2). The Thinhope and Glendue Burns have very similar geology: mainly Carboniferous Mudstone, sandstone and Limestone. Microgabbro is also evident on Thinhope Burn. The Knar Burn geology comprises Limestone, sandstone, siltstone and mudstone. The bedrock in the three catchments is overlain by Pleistocene glacial diamict that has been modified by solifluction processes on slopes. In the headwaters of each sub-catchment, peat overlays the diamict to depths of up to 2 m. In terms of geological controls, a single fault is evident on Thinhope Burn around 500 m downstream of the confluence of the 2nd order Feugh Cleugh. Two notable faults are evident on the Knar Burn in close proximity to one another immediately downstream of the confluence of the Knar Burn with the Gelt Burn. No faults are evident on the Glendue Burn. Land-use in the catchments is predominantly moorland in the headwaters with some rough grassland grazed by sheep. On Thinhope Burn upstream of Burnstones bridge (<1 km from the confluence with the South Tyne), interception is limited to that afforded by heather, bracken, and grasses, with some riparian forest evident downstream of Burnstones. A small coverage of predominantly riparian forest is found on the Glendue (<15% of catchment area) and Knar Burn (<3% of catchment area). Catchment hydrology is influenced by natural pipe drainage in the peat, and is also assisted through an artificial field drainage system, locally known as 'grips,' cut into the peat down to the diamict, which were installed between the 1960s and 1980s in the belief that they would benefit both livestock and grouse. Although the three tributary sub-catchments to the South Tyne under investigation in this study were not gauged, flow data exists for the South Tyne itself at Featherston approximately 4.5 km downstream of its confluence with the Glendue Burn (Figure 1A). Peak flow data are of key interest in this study, and annual peak flows since 1966 are plotted in Figure 3. Between 1966 and 1993 the maximum flow was 310 m^3s^{-1}. Since 1993 there have been seven years where peak flows have exceeded this figure.

Figure 1 Study Catchments; A) South Tyne catchment and three sub-catchments at the centre of investigation. Tributaries to Thinhope Burn are indicated (M - Mardy's Cleugh; F – Feugh Cleugh), and Knar Burn (G – Gelt Burn); B) DEMs for neighbouring Knar, Thinhope and Glendue Burns. The 5km^2 NIMROD radar cells are overlain and the 24 hr rainfall totals are indicated in the corner of each cell.

Figure 2 Photos of A) Glendue Burn (July 2008), B) Thinhope Burn (June 2004) and C) Knar Burn (July 2008)

Figure 3 Annual peak flow data for the South Tyne and Featherstone, station 23006, (nrfa.ceh.ac.uk).

Notably the peak flows in 2004, 2011, 2012 and 2015 all exceeded 400 m^3s^{-1}, with the 2012 peak flow exceeding 500 m^3s^{-1}. There is a strong suggestion that the change in hydrology is linked to the current wet phase in UK climate, that is predicted to be most pronounced in upland areas in the winter months (Dadson et al., 2017). The 2007 summer event discussed in this paper did not appear to produce significant catchment-wide flooding on the South Tyne, probably due to the localised nature of the storm (Figure 1B), hence does not appear as a notable maxima. However, it is likely that the increasing magnitude and frequency of extreme events shown in the South Tyne peak flow data, is influencing geomorphic processes throughout the catchment.

Morphometric details of the three catchments are provided in Table 2. The indices are included in the Table, mainly due to their potential influence on the flood hydrograph and its attenuation through the catchments, and the possible implications of these factors will be discussed later in the paper. Both Thinhope and Glendue Burns are 3rd order, whereas the Knar Burn is a 4th order stream prior to its junction with the South Tyne. The Knar Burn has the largest catchment area, perimeter, stream and catchment length, catchment width, form factor and circularity ratio, followed by Thinhope and then Glendue Burns. It is however the smaller Glendue catchment that has the greatest channel slope, drainage density and elongation ratio, followed by Thinhope and then the Knar Burn. There are some differences in bed surface grain size, as assessed through Wolman (1954) grid sampling, with the Knar Burn displaying the coarsest bed surface sediment, followed by the Glendue Burn and then Thinhope Burn (Figure 2). It should be noted that the grain size information is limited to single reaches on the three streams, and no information is available on the full variability along the full length of each of the study streams.

Table 2 Morphometric characteristics of the study catchments. The grain-size information reported are for single reaches located in the vicinity of Knarburn: 54°51'34.48"N, 2°31'36.37"W; Thinhope Burn: 54°52'46.59"N, 2°31'15.70"W; Glendue Burn: 54°54'3.62"N, 2°31'6.30"W

The summer 2007 flood; frequency estimation using lichenometry

On the 17th, 19th, and 23rd of July 2007, a series of convective storm cells caused localised flooding around the South Tyne catchment. Rain-gauge and river flow data are unavailable for the three study catchment's themselves; however, NIMROD rainfall radar data were available (Figure 1B), and revealed a highly localised storm situated in the headwaters of Thinhope and Glendue Burns on 17 July. The event started at around 16:00 British Summer Time and lasted approximately 2 hours. The 24 hour rainfall for a 5-km^2 radar grid cell located in the headwaters was 236 mm, and returned a maximum hourly rainfall of 30 mm h^{-1}. Following the event flood marks, including dead vegetation; grass, sedges, bracken, calluna, fragments of silt, and marks on trees, were used to estimate peak discharges, using the Manning-Strickler formulae (Manning, 1891). Probable discharges equated to 60 m^{3}s^{-1}, 6 m^{3}s^{-1} and 19 m^{3}s^{-1} for Thinhope Burn, Glendue Burn and Knar Burn respectively, with the ranges of the estimates shown in Table 3. Probable specific peak discharges for Thinhope Burn were 5.5 m^{3}s^{-1} km^2, substantially greater than the neighbouring Glendue (1.3 m^{3}s^{-1} km^2) and Knar Burn (1.1 m^{3}s^{-1} km^2) catchments, with indicative ranges around these estimates shown in Table 3. To give some context, the Thinhope Burn specific peak discharge exceeds the value of 2.7 m^{3}s^{-1} km^2

reported by Carling (1986) for Langdon Beck and fell within the range (2.4 and 10 m^3s^{-1} km^2) reported by Harvey (1986) for the Howgill event.

Table 3 Peak discharge estimations and approximate runoff rates for the study sites for the 17th July 2007 flood (adapted from Bain et al., 2017)

Comparing the 2007 event with Thinhope Burn's flood history

It is recognised that caution should be applied when estimating recurrence interval, due to the non-stationarity of river flows over both decadal and centennial timescales, due to climate and land-use changes (Milly et al., 2008). However, old flood deposits (cobble-boulder bars, sheets and splays, and boulder berms and lobes) dated prior to the 2007 flood, using the lichen *Huilia tuberculosa* (Macklin et al., 1992), and data collected post flood in 2007 (Milan, 2012), allow an extreme event recurrence interval to be estimated for Thinhope Burn, based on evidence for 22 events since 1766. Macklin et al. (1992) also measured the grain-size of the ten largest clasts on the berms considered in their lichenometric analyses, giving a surrogate for flood magnitude. The D_{50} of ten largest clasts measured from fresh boulder berm deposits following the 2007 event was 730 mm (Milan, 2012), and when compared with dated flood deposits it was evident that events of a similar magnitude to 2007 had only occurred twice since 1766, with major event's occurring in 1766 (D_{50} = 740 mm), and in 1929 (D_{50} = 730 mm), suggesting a recurrence interval for the 2007 flood of 1 in 80 years.

Methods

Morphodynamic modelling

To achieve the study aims, a cellular landscape evolution model (CAESAR-Lisflood) was employed (Coulthard et al., 2013; Van de Wiel et al., 2007). CAESAR has previously been shown to be an effective tool to explore differential catchment-scale geomorphic response to environmental change over the Holocene in upland Britain (Coulthard et al., 2005). CAESAR-Lisflood combines a hydrological and hydraulic flow model that operates on a sub-event time step, simulating the transport of grain size mixtures, morphological changes and slope processes. TOPMODEL is used to simulate catchment-scale hydrological processes (Beven and Kirkby, 1979), whilst a hydrodynamic 2D flow model, based on the Lisflood FP code (Bates and De Roo, 2000), that conserves mass and partial momentum, and simulates in-channel hydraulic processes, is used at the reach-scale. Bedload sediment transport is calculated using Wilcock and Crowe's (2003) equation, well suited to the grain size mixtures found in gravel-bed rivers.

Newtonian or non-Newtonian flow?

Newtonian flow conditions are assumed for sediment transport in the modelling, although it is acknowledged that flash floods can generate non-Newtonian conditions. Interpretation of sediment deposits following flash floods in upland and mountain river systems can be problematic. Deposits resembling the form and sedimentary structure found on Thinhope Burn (Macklin et al., 1992), have been attributed to flows with high sediment loads, variously defined as 'debris torrents' (Miles and Kellerhals, 1981), 'bedload' (Iseya et al., 1992, and 'hyperconcentrated' (Pierson and Scott, 1985; Scott, 1988) flows. Carling

(1987) concluded that berm deposits on the West Grain River, North Pennines, UK, resulted from debris torrents, as opposed to debris flow deposits (Costa, 1984). Debris flows may be strongly non-Newtonian whilst debris torrents tend to be transitional or Newtonian in character, depending on the sediment concentration (Pierson and Costa, 1987). Carling (1989) also working on north Pennine streams, noted that suspended sediment loads were low even during high flows, typically less than 100 mg 1^{-1}, and contained little clay (Carling, 1983). Furthermore, high magnitude streamflows in catchments >10 km^2, can be Newtonian in character even with concentrations of gravel and boulders of up to 50% (Rodine and Johnson, 1976; Pierson and Costa, 1987; Carling, 1989). Carling (1987; 1989; 1995) further indicated that berms tended to be created in flow separation zones, where their presence may provide a useful indicator of Newtonian as opposed to non-Newtonian flow conditions at the time of formation. In addition, imbricate structures can be associated with debris torrents (Carling, 1987). Following the 2007 event on Thinhope Burn, although there was some limited evidence of poorly sorted deposits, suggestive of non-Newtonian flow conditions for a short period on the hydrograph, the morphological and textural evidence pointed more strongly in favour of Newtonian flow conditions. For example, there was clear evidence of berm deposition in flow separation zones on the inside of meander bends (Figure 4A, B), and linear openwork deposits on the banktop (Figure 3C); both features identified by Carling (1987; 1989). Imbrication and cluster formation involving some of the coarsest clasts was also clear (Figure 3B,D,E).

Figure 4. Morphological and sedimentological characteristics of deposits in the Thinhope Burn catchment, following the July 2007 flood event; A) and B) Berms

deposited on the inside of meander bends on Thinhope Burn, C) Linear boulder ribbon deposited on floodplain in a steeper section of Mardy's Cleugh, D), E) and F) Boulder cluster bedforms; note the Nokkia 3410 mobile phone for scale.

Catchment-scale runs

For this investigation CAESAR-Lisflood was initially run in catchment mode, using a 10 m resolution DEM, where the three catchments were modelled separately. Typically there is an initial period of high bedload transport and rapid morphological adjustment as the model domain evolves in response to the imposed initial and boundary hydrodynamics, and model parameterisation (e.g. Bras et al., 2003; Kleinhans, 2010). A period of morphodynamic 'spin-up' was employed to overcome the initial high sediment delivery, whereby the model was run with a 10 year hourly rainfall series from Keswick (latitude 54º 36.0" N, longitude 3º 31' 08.0" W). In addition the 10 year period also facilitated an assessment of long term responses to wetter climatic periods, and the differences in sediment yield between the three study catchments. Although Keswick is situated to 50 km west of the South Tyne catchment, it was thought likely to exhibit broadly similar rainfall characteristics related to the dominant UK weather patterns, i.e. frontal rainfall. The end-point catchment DEM was then used as the start-state DEM to run local, hourly 5 km^2 NIMROD rainfall radar for 11^{th} – 24^{th} July 2007, to investigate geomorphic response to the July 2007 floods, and enable spatial variations in rainfall to be established over short distances between the neighbouring catchments (Figure 1B).

Comparisons of geomorphic effectiveness and threshold exceedance, between the three catchments were investigated by scaling the magnitude of the 11th – 24th July 2007 series to simulate the effects of different magnitude events (typically 0.25, 0.5, 0.75, 1.0, 1.5 of the rainfall). Comparisons of catchment-scale response (geomorphic effectiveness) to varying flood magnitudes were made through comparisons of geomorphic work (*sensu* Wolman and Miller, 1960), quantified through an examination of catchment cumulative sediment efflux initially over a 10 year period (1997-2007). Geomorphic work was also quantified in the same manner for the scaled runs of the 2007 event, permitting an analysis of the effects of event magnitude upon geomorphic work and identification of threshold exceedance. Through analysis of catchment sediment output it was hoped to link any increases in sediment transport rate to sediment transport initiation in the channel, and releases from stores held in old flood deposits and terraces, and infer threshold discharges for these.

Reach-scale modelling

Further attention was directed to the response at the reach-scale for Thinhope Burn, that showed responsive behaviour to the July 2007 event (Figure 5), allowing a closer examination of sediment transport processes and geomorphic work, and a comparison with quantitative observations of morphological impacts reported in Milan (2012). Here, CAESAR-Lisflood was run in reach mode this time using a 2 m LiDAR DEM and the discharge and sediment efflux from the catchment scale run. A uniform Mannings n of 0.032 was used to represent grain roughness effects and was calculated using Vischer and Hager's (1998) equation

$$n = \frac{(D_{50})^{1/6}}{21.1} \quad (1)$$

where the D_{50} was based on empirical measurements (Wolman, 1954) of grain size in berms, lobes and bars, with form roughness accounted for in the DEM. It is acknowledged that some workers have represented spatial roughness variability within the model domain to represent differences between floodplain and channel elements for example (e.g. Thompson and Croke, 2013; Quesada-Román et al., 2020). However as spatial patterns of roughness change over the course of a large flood, with parts of the floodplain stripped, new gravel deposited onto the floodplain and old flood deposits re-worked, pre-flood spatial roughness is not likely to reflect the condition at peak flow. Most of the studies that have used spatial roughness have applied it to situations where the floodplain has remained relatively stable (e.g. Werner et al., 2005; Wong et al., 2015). For the spatial roughness approach to be successful in the current case, the model domain would need to make spatial roughness updates as the roughness changes over the course of the event, which for CAESAR-Lisflood is currently not possible. In a companion paper (Milan and Schwendel, 2021), a validation and sensitivity exercise ran for a discharge of 60m^{3}s^{-1} on a 500 m reach of Thinhope Burn, where the Mannings *n* roughness coefficient was varied between 0.02 and 0.06, found n=0.03 to provide a close match between simulated water surface elevations and trashline elevations measured using RTK-GPS soon after the July 2007 flood. Using a uniform roughness based upon median grain size, empirically-derived from various units throughout the reach including bars, berms and splays, therefore provided a realistic roughness estimate for the reach. The empirically-derived grain size distribution was also used for sediment transport in the model. The model was run on a 3 km reach, however attention is focused on the same 500 m reach reported in Milan (2012), to aid comparison with empirical field analyses.

Figure 5 The 500 m reach of Thinhope Burn where detailed morphological changes have been documented (see Milan, 2012; Milan and Schwendel, 2019; Schwendel and Milan, 2021), and used for reach-scale morphodynamic modelling in this paper (source: Google Earth Pro, 2021).

The depth-average velocity and depth output rasters from the simulations were converted to boundary shear stress (τ_b) using

$$\tau_b = \frac{\rho g V^2 n^2}{y^{\frac{1}{3}}} \ (\mathrm{Nm^{-2}}) \qquad (2)$$

where V is depth-averaged velocity, ρ is water density, g is gravitational acceleration, n is the Manning's roughness coefficient, and y is water depth over each pixel.

Results

Catchment sediment efflux

It is clear that Thinhope Burn produces significantly more sediment over the study period, despite it displaying lower discharges than the Knar Burn catchment, and possibly highlighting the sensitive nature of this catchment (Figure 6). Predicted discharges are greater for the larger Knar Burn followed by Thinhope and then the smallest catchment, the Glendue Burn. The discharge series reveal flood rich periods between 1998 and 2001, and 2005-2008. Inspection of the Thinhope discharge series (Figure 6C) reveal several peaks that exceed the 2007 summer flood peak estimate (Milan, 2012), and therefore suggest that the Keswick rainfall series, was higher than that experienced locally. For the Thinhope Burn simulations, this resulted in notable discharge peaks of 81, 103 and 135 m^3s^{-1} seen in the series (Figure 6C). Simulated discharges are also likely to be overestimated for Knar Burn and Glendue Burn (Figures 6B, D). Although it is acknowledged that flows are overpredicted, this did not present an issue for the exploratory comparison of the effects of different magnitude flows on geomorphic work, at the center of this paper.

Figure 6 Time series plots showing A) cumulative sediment efflux from catchment scale runs for 1998-2007, simulated discharge for the B) Knar Burn, C) Thinhope Burn, D) Glendue Burn.

Estimates of total sediment efflux from the simulations allow a comparison to be made concerning the amount of geomorphic work undertaken by the three neighbouring catchments. Total simulated sediment outputs for Knar, Thinhope and Glendue Burns were 5172 m^3, 18801 m^3, and 349 m^3 respectively. The 1998-2001 flood-rich period is associated with the sharpest rises in sediment yields over the 10 year period, for all three sub-catchments. Relatively low magnitude events occur between 2001 and 2005, and this is reflected in low sediment yields during this period, represented by flatter trajectories on the cumulative plots in Figure 6A. The largest events towards the end of the series (between 2005-2007) result in a marked increase in sediment output for the

Thinhope catchment, with a more damped response shown in the Glendue and Knar catchments.

Sediment efflux comparison for the summer 2007 floods: geomorphic effectiveness and identification of threshold exceedance

Over the 14 day period between 11^{th}-24^{th} July 2007 there were two peaks on the hydrograph, the major peak occurring at 2 am on the 18^{th} July and a minor peak on 20^{th} July 2007 (Figure 7). The rainfall events for this period were scaled to simulated discharges of different magnitudes, and the scaling and discharge peaks are indicated in the Figure legends. The aim of this procedure was to examine differences in sediment outputs (geomorphic work), and thresholds for sediment mobilisation between each sub-catchment. The discharge hydrograph using unscaled (1.0) rainfall radar input for Thinhope (see blue line on Figure 7A) shows a discharge peak of 90 m^3s^{-1}, which is greater that the previous reported estimate of 60 m^3s^{-1} (Milan, 2012), suggesting either that the TOPMODEL rainfall runoff component of CAESAR-Lisflood is overestimating discharge, or previously reported estimates for peak discharge using post-flood trash line elevations to derive hydraulic radius data for input into the Manning Strickler equation, underestimated discharge. Either way it is important to point out that does not affect the analysis and interpretations made in this paper, as it is the comparative geomorphic work undertaken by the study catchments under a range of peak flow scenarios that is the focus of this investigation.

Figure 7 Results from CAESAR-Lisflood simulations over the 14 day period between 11^{th}-24^{th} July 2007, following spin-up: A-C) Hydrographs produced using scaled rainfall inputs for the three study catchments, D-F) cumulative sediment efflux from the scaled model runs.

For Thinhope Burn, sediment output shows a clear stepped appearance, where each of the steps are related to the two hydrograph peaks. These steps, particularly evident for the larger events for all three sub-catchments (Figure 7D-F), result from relatively sudden increases in sediment transport, and hence may be inferred as being indicative of intrinsic thresholds being crossed, such as sediment stored in the bed and bars, and old flood deposits stored in boulder bars, splays, lobes and berms. Although sediment transport takes place in response to the main flood peak for the 0.25 and 0.5 scaled runs, there is a marked increase in sediment transport for the 0.6 run. Surprisingly there is not such a marked further increase in sediment transport for the peaks on the 1.0 and 1.5 scale runs. This may suggest that a sediment transport threshold is reached somewhere in the flow range, possibly reflecting sediment availability (and then exhaustion) in berms and lobes situated on lower terraces within the Thinhope valley. Although sediment transport increases slightly on the second hydrograph peak for the 0.6 run (where 14 m^3s^{-1} was reached on the 2nd peak), a more marked increase is shown for the 1.0 and 1.5 runs, where 39 m^3s^{-1} and 85 m^3s^{-1} were reached on the secondary peaks respectively. This may reflect the flow reaching a higher terrace level and reworking of these areas.

The other two catchment runs do not allow as much insight into threshold exceedance. For the Knar Burn, sediment transport is only really notable for the three higher simulations (0.75, 1.0 and 1.5 scale runs), and again increases are associated with the primary and secondary hydrograph peaks (Figure 7B,E). For

Glendue Burn, sediment transport is only notable for the highest flow simulation (1.5 scale run), with the slight rises associated once more with the primary and secondary hydrograph peaks. Less significant sediment efflux is shown for the 1.0 scale run, and only associated with the primary discharge peak (Figure 7C,F).

Comparison of geomorphic effectiveness undertaken in study catchments

To compare the geomorphic effectiveness undertaken by the three neighbouring catchments in response to the summer 2007 event, the geomorphic work undertaken is quantified through comparing total sediment outputs plotted against the peak discharges for the different model runs using the scaled rainfall series (Figure 8). The Thinhope Burn curve sits farthest left of the three, indicating greater sediment efflux, and hence geomorphic work, for a given discharge in comparison to the neighbouring catchments. The steeper curve also suggests greater responsiveness to discharge increases than the two neighbouring catchments. However, in contrast to the cumulative sediment efflux totals shown earlier in Figure 6, it is the smaller Glendue Burn catchment that shows greater geomorphic work compared with the largest catchment of the three the Knar Burn. Comparative geomorphic effectiveness at the catchment-scale may be examined by comparing the geomorphic work undertaken by the 60 m^3s^{-1}, equivalent to the previously reported flood peak seen on Thinhope Burn (Milan, 2012), that resulted in a total sediment efflux of 575 m^3. This was over seven times that predicted for Glendue Burn and nearly nine times greater than that shown for the Knar Burn.

Figure 8 Total sediment efflux plotted against peak discharge for each scaled run, over the14 day period between 11th-24th July 2007, for the three study catchments.

Comparison of reach-scale spatial hydraulics and morphological impacts for varying flood magnitudes

For all the simulations shown, CAESAR-Lisflood produces a net sediment loss from the reach (Figure 9). Observations of bedrock over the full length of Thinhope Burn both before and after the 2007 event did not reveal any channel bed exposures, and was only evident as lateral confinement, with bedrock appearing occasionally at slope channel coupling zones (e.g. Figure 10C). The simulated vertical changes are therefore assumed to be acting on a fully alluvial channel. As may be expected, greater morphological changes take place with greater flow peaks, in response to the greater hydraulic forces exerted on the bed. A 4 m^3s^{-1} event generates boundary shear stresses generally below 150 Nm^{-2}, resulting in limited bedload transport, with net sediment erosion of 31 m^3 and vertical changes in the range -0.33 m to +0.10 m. Greater peak shear stresses generally around 350 Nm^{-2} are found at the 27 m^3s^{-1} peak, which is also capable of inundating a larger area of bed and filling a small paleochannel towards the downstream end of the reach. This flow produced vertical scour and fill in the range -0.63 m to + 0.49 m, and resulted in net erosion of 71 m^3. The 60 m^3s^{-1} event produced very strong contrasts in shear stress; with the main thalweg showing shear stresses of up to around 650 Nm^{-2}, however the inside of meanders and some channel margins showed comparatively low shear stresses of <100 Nm^{-2}. A second paleochannel at the head of the reach is activated at this discharge. This flow peak resulted in vertical scour and fill in the range -0.54 m to +1.70 m, with net sediment loss of 130 m^3. The 90 m^3s^{-1} event inundated wider parts of the valley floor and again results in clear spatial contrasts in shear stress with peaks around 750 Nm^{-2}. This flow peak resulted in vertical scour and fill in the range -1.87 m to +2.41 m, and net erosion of 847 m^3, with some evidence of sediment wave stalling and bifurcation at the head of the reach, and berm formation elsewhere. The 236 m^3s^{-1} event once again displayed marked spatial contrasts in hydraulics across the reach, demonstrating the potential for extreme bedload transport in some areas with peak shear stresses again around 750 Nm^{-2}, however areas of low shear stress still exist even at this discharge; allowing the potential for lower sediment transport rates and perhaps bedload stalling to take place. Many of the zones of peak shear stress at high flow do not always map on to scour zones, suggesting that these areas may fill with sediment on the falling limb of the hydrograph. The DoD in this 'severe' scenario showed vertical scour and fill in the range -2.14 m to +4.99 m, and net erosion of 991 m^3.

Figure 9 Reach-scale CAESAR-Lisflood output for Thinhope Burn: A) geomorphological work at the reach-scale using end-point rasters for DoD output for five of the different flow peaks generated from scaled rainfall data in the catchment-scale runs; B) shear stress rasters taken at each of the five flood peaks. N.B. Aerial photos showing actual response of the study reach to the 2007 event are shown in Figure 5.

Figure 10 Main sediment stores and sources on Thinhope Burn: A) boulder berms perched on terraces; B) eroding slope-channel coupling zones supplying till (base unit) and alluvium (near surface unit); C) tributaries; D) eroding terraces.

Hydraulic distribution

One way of further analysing the potential of different flow magnitudes to undertake geomorphic work is to interrogate the shear stress values for each raster pixel from the reach for each flow simulation peak (Figure 9), and to plot these as population distributions (Figure 11). When it comes to quantifying geomorphic effectiveness, shear stress has been noted as being one measure of 'cause' (Lisenby et al., 2018), that provides a very precise measure of event magnitude. The 4 m^3s^{-1} event shows a very narrow range of shear stresses with the mode of around 150 Nm^{-2}. Shear stress distributions for the 27 to 236 m^3s^{-1} flows all show some degree of bimodality, with common peaks shown at the lower end of the distribution at around 50 Nm^{-2}, indicative of shear stresses in areas where water has spilled out of channel, and higher secondary peaks reflecting in-channel processes. There is slightly more spread for the 27 m^3s^{-1} flow peak, with primary mode of just under 350 Nm^{-2}. The population distribution of shear stress for the final three simulations (60, 90 and 236 m^3s^{-1}) all produce very similar distributions, with no marked increase in the mode (~450 Nm^{-2}) at the higher end of the shear stress distribution. The proportion of shear stresses >450 Nm^{-2} for the 60 and 90 m^3s^{-1} simulations is almost identical (33% and 34% respectively), greater than the proportion exhibited for the 236 m^3s^{-1} simulation (25%). This possibly suggests that flows in excess of 60 m^3s^{-1} may not able to exert significantly greater energy on the channel boundary, and hence may only achieve more work as a result of the flow peak being in excess of that required to mobilise bedload for a longer period, or through the fact that a greater area is inundated at progressively higher stages. It is argued therefore that flows significantly in excess of 60 m^3s^{-1} appear unable to 'trip' any additional shear stress thresholds for sediment transport. It should be noted that the modelling here assumes Newtonian flow conditions and an available supply of sediment. However, if flows were to become non-Newtonian in nature, then it would be feasible for greater sediment transport and geomorphic work as a result.

Figure 11 Population of shear stress for different flow peaks, using the values from each pixel from shear stress raster (Figure 9) generated using depth and velocity outputs from CASAER-Lisflood outputs and through the application of Equation 1.

Discussion

Geomorphic Effectiveness

The approach adopted in this paper has been to use sediment efflux (geomorphic work) as a measure of geomorphic effectiveness (Wolman and Miller, 1960) rather than landform modification (Wolman and Gerson, 1978). Causal factors driving effectiveness at the catchment-scale include 1) duration and intensity of rainfall, and 2) discharge. The dominant nature of rainfall events impacting the study catchments is winter frontal rainfall, delivering broadly similar rainfall magnitudes and frequencies. However, the 2007 event was induced by localised, intense convectional storm cells, as highlighted in the 24 hour rainfall totals (Figure 1B). Hence localised convectional events, more commonly occurring during the summer months, can result in very localised and catchment-specific flooding and enhanced geomorphic effectiveness. However, CAESAR-Lisflood modelling (Figure 8) clearly indicates that Thinhope Burn generates more geomorphically effective flood peaks for a given discharge, resulting in greater geomorphic work in comparison to the neighbouring catchments. Shear stress drives effectiveness at the reach-scale, where analysis indicates that discharges significantly in excess of 60 m^3s^{-1}, do not appear capable of achieving higher modal values of shear stress. Grain size and morphological form is likely to be fundamentally linked to the energy spectra within the catchment. Hence 60 m^3s^{-1} could be seen as a threshold discharge capable of transporting every available grain size in the reach and modifying available forms (bars, berms, lobes and splays).

DoDs shown in Figure 9, indicate increasing erosion and deposition volumes (geomorphic work) throughout the simulated flow range. Net erosion is seen for all the simulations however, which suggests efficient removal of sediment from the reach. It is noteworthy that empirical resurvey data for Thinhope Burn indicated initial net deposition following the 2007 event (Milan and Schwendel, 2019; Milan and Schwendel, 2021), however with periods of net erosion in the years that followed. Although the 60 m^3s^{-1} simulation contrasts with the net sediment delivery calculated using empirical pre- and post-event field re-survey data, the gross pattern of berm deposition on the inside of meanders was similar to that reported in Milan (2012). Furthermore, ten years after the event, the reach has remained more active compared to the pre-disturbance condition (Milan and Schwendel, 2021). Observations also reveal a wider channel in a more active unvegetated valley floor, with a wandering channel morphology in comparison to the narrow single-thread sinuous stream that was in evidence prior to the 2007 event. Hence it is argued here that Thinhope Burn has shown 'river change' (Brierley and Fryirs, 2005); a 'wholesale shift to a different state' (*sensu* Brierly and Fryirs, 2016, p825), triggered by the wetter climatic regime currently linked to the wetter phase in the Britains climate (Dadson et al., 2017). It could be further argued that future climate change, in the form of a trend of increased winter precipitation (for England and Wales) evident since the late 1700s (Dadson et al., 2017), has pushed the Thinhope system close to exceeding extrinsic thresholds, and increased system sensitivity. Evidence of response to longer term climate forcing with phases of incision thought to be coincident with cooler wetter periods in Britains climate, are also well documented for Thinhope Burn (Macklin et al., 1992).

Boundary and flux conditions

Brierley and Fryirs (2016) 'river evolution diagram' provides a useful conceptual framework for understanding channel response to disturbance on Thinhope Burn, highlighting the hierarchical nature of imposed 'boundary' and 'flux' boundary conditions. Boundary conditions are large and change over longer timescales due to extrinsic factors like climate change and geological controls on topography, base level and valley confinement. They impose threshold conditions that dictate smaller, more transient flux boundary conditions, that include interactions between water, sediment and vegetation, and which produce different channel types. The total range of energy conditions set by the imposed boundary limits determines the range of channel types that may develop in a particular valley setting.

For Thinhope Burn, imposed boundary conditions such as catchment-scale morphometric attributes (Table 2) could theoretically explain differences in geomorphic response. The larger of the three catchments is the Knar Burn; a 4th order stream prior to its junction with the South Tyne, and as a consequence it could be argued that this catchment could produce the highest flow magnitudes and sediment efflux. Average valley slope is greatest in the smallest catchment Glendue Burn, and this catchment has the greatest stream density which should produce more rapid runoff, more 'pointed' hydrograph peaks. Both the Knar Burn and Thinhope Burn have very similar average slopes, and are both 3rd order streams. More circular catchments with a higher drainage density may induce more rapid translation of rainfall and result in higher flood peaks for a given rainfall event. The most circular and least elongate catchment is the Glendue Burn, followed by Thinhope and then Knar Burn. However, whichever morphometric parameter is considered, it appears that Thinhope falls somewhere in the middle, and hence these catchment-scale morphometric parameters do not appear to offer a good explanation for enhanced effectiveness shown by Thinhope Burn. The bedrock geology of the three catchments is also broadly similar, and qualitative observation suggests that existence of faults, evident on the Thinhope and Knar Burns does not appear to have a major influence on local channel morphology or long profile. However, more detailed empirical analysis of geological influence upon the three catchments, may elucidate further possible geological influences upon fluvial processes.

Sensitivity

The results in this paper primarily inform on geomorphic effectiveness as they concentrate on simulated sediment efflux, however some conclusions can be drawn with regards to geomorphic sensitivity. It seems clear that for the three catchments to become fully activated, the thresholds required to activate the key sediment stores in the catchment (boulder berms, lobes, splays, and terraces) need to be attained. The stability of fluvial landforms is a function of the temporal and spatial distributions of the resisting and disturbing forces, the 'propensity for change', and is diverse and complex (Brunsden, 1990; Downs and Gregory, 1993; 2004; Phillips, 2009). The disturbing forces are those operating within imposed boundary conditions (Brierley and Fryirs, 2016), that disrupt the geological, hydrological and morphological framework of a system, and can include climate change, tectonic controls, anthropogenic factors such as land-use and biotic factors (Brunsden, 2001). 'Landscape' change takes place as a normal process–response function to an imposed change in regime and involves sediment transport, morphological evolution and structural rearrangement as thresholds are crossed within imposed flux boundary conditions (Knox, 2000; Brierley and Fryirs, 2016). Resisting forces of a system relate to ability of the system to resist threshold exceedance and hence retain its landform assemblage, following a disturbance. These forces include 1) Strength resistance, 2) Morphological resistance, 3) Structural resistance, 4) Filter resistance, and 5) System state resistance (Brunsden, 1993a,b). Some of these factors may explain the greater geomorphic effectiveness of Thinhope Burn. Grain-size information available for single reaches of the three streams indicates broadly similar characteristics, but with both the Knar and Glendue Burns showing slightly coarser bed surface sediments (Table 2). This results in slightly greater critical threshold shear stresses for mobilisation for the Knar and Glendue Burns (Table 2), and renders them slightly less sensitive to change in comparison to Thinhope Burn.

Thinhope Burn has much greater form roughness in comparison to its neighbours. The valley has a distinctive 'inherited' morphology from phases of climatically driven incision over the Holocene, which produced a set of terraces, coupled with depositional flood units (berms, splays and lobes), deposited by floods since the late 1600s (Macklin et al., 1992). Morphology influences landscape sensitivity either by concentrating or diffusing the application of stress, and it would seem feasible that terraces and berms present loci for the concentration of stress within the system.

The strength resistance offered by the key sediment sources in the Thinhope valley (berms, lobes, splays and terraces), is also likely to be important for determining sediment efflux and hence geomorphic effectiveness (Figure 10). Brunsden (2001) notes the importance of the physical properties of the materials making up morphological units; the strength and erodibility of the morphology and the way in which the clasts respond to stress in either a liquid, plastic or brittle way as important in determining geomorphic response. The properties of sediment deposits also influences the propensity for change (Downs and Gregory. 1993; 2004). Open-work unstructured flood deposits have a low physical strength due to the lack of; a) fine sediment reduces the binding effect between framework clasts (Reid et al., 1985; Allan and Frostick, 1999; Haynes and Pender, 2007), b) imbrication (Komar and Li, 1986; Petit 1990), and c) bed structures such as clusters (Brayshaw 1985; Hassan and Reid, 1990), that have been shown to reduce the threshold shear stress required for mobilisation and increase sediment flux (Oldmeadow and Church, 2006). For Thinhope Burn, Macklin et al. (1992, pp 636) comment on the 'open-work clastsupported' structure of the boulder berms, highlighting a lack of interstitial matrix, and the 'weaker fabric' of boulder lobes in comparison to the berms. Pre-2007 flood catchment walks, revealed similar flood deposits with a similar structure were evident in all three catchments. However, these were more prevalent on the Thinhope Burn and hence most likely provided greater sediment supply from this source compared to the neighbouring catchments. In addition, boulder berms and lobes deposited on the falling limb of the hydrograph are unlikely to see any inter-flood reworking, important for delivering fine sediment and developing bed structure (Reid and Frostick, 1984; Reid et al., 1985; Ockleford and Haynes, 2013).

Structural resistance; the 'design' of a system, its components (and their juxtaposition), topology, links, thresholds and controls (Brunsden 1993a,b), may also play a role in determining geomorphic effectiveness on Thinhope Burn. Two further sub-factors are important here 'location sensitivity' (which also relates to connectivity ca. Fryirs, 2017) and 'transmission resistance' (Brunsden, 2001). On Thinhope Burn, the main sediment stores in the 3rd order main valley (berms and terraces), are located in close proximity to the contemporary channel (Figure 10A), and as soon as threshold discharge and stage is reached whereby these sediment sources may be accessed by hydraulic processes, then these may become mobile; it just requires a flood stage capable of reaching the sediment stores. Furthermore, it seems feasible that once boulder berms become mobilised at the head of the Thinhope 3rd order channel system, coupled with fresh supply predominantly from the 2nd order part of the stream network, then morphological change initiated at the head of the 3rd order system has the potential to rapidly propagate further change downstream. Hence, when berms become mobilised at the head of the system, a chain-reaction of process-form feedbacks is transmitted downstream; with sediment waves triggering flow diversions and avulsions.

In addition, Thinhope Burn may have historically received more localised intense convectional rainfall events in comparison to its neighbouring catchments, due to local orographic effects (e.g. Napoli *et al*., 2019). The frequency and duration of disturbances relative to geomorphic relaxation times is also known to be important (Phillips, 2009). The past history of floods (magnitude, frequency and sequencing of events), in turn leads to the morphology and structure that is inherited by the next potentially geomorphologically effective event (Newson 1980; Beven, 1981; Lisenby et al., 2018). Every system receives a unique pattern of 'impulses of change' and 'formative events' (Brunsden, 2001); no two catchment systems are likely to receive the same number, sequence, frequency, duration and magnitude of events. This 'System State resistance' would limit the ability of Thinhope Burn to recover in comparison to its neighbours as the ratio of geomorphically effective events to recovery time would be larger, thus promoting change persistence in the landscape (Brunsden and Thornes, 1979; Thomas, 2001).

Future management of upland river catchments

Since the early 1990s in the South Tyne catchment, there has been a change in the magnitude and frequency of floods with peak discharges in excess of 300 m^3s^{-1} (Figure 3). The change in the magnitude and frequency of large flood events is one possible factor acknowledged as triggering threshold exceedance in river systems (Beven, 1981; Nolan *et al*., 1987; Gupta and Fox, 1974;

Newson, 1980; Kochel 1988; Magilligan, 1992; Kale et al., 1994; Costa and O'Connor, 1995; Milan et al., 2018). This undoubtedly will influence geomorphic processes within the larger Tyne catchment as a whole, and those sub-catchments that are more sensitive (e.g. Thinhope Burn) are likely to show responsive behaviour, manifest as a relatively dramatic response in terms of sediment transport and morphological change (Figure 9). The catchment-scale morphodynamic modelling presented in this paper suggests that when sensitive catchments are activated they can mobilise and deliver significantly more sediment than similar sized resilient catchments. Sensitive upland catchments when activated, therefore may result in increased flood risk further down the river system as a consequence of sediment delivery from upstream. Current flood-risk management strategies in such circumstances however make no geomorphologically-underpinned assessment of the situation, and often focus instead on 'reactive' removal of gravel and clearing of vegetation, as this is perceived as a significant causes of local flooding (e.g. McCall and Webb, 2019). It is well established that removal of gravel often deposited as newly created bedforms, may exacerbate channel instability potentially propagating both up- and downstream (Kondolf, 1997); increasing system sensitivity (Sear and Newson, 2003), preventing a return of 'endangered' natural morphologies (Heritage et al., 2022), and potentially damaging instream riverine ecosystems (Hauer et al., 2016).

Future sediment management in upland catchments must be underpinned by geomorphology to guarantee the preservation or return of 'rare' channel morphologies (Heritage et al. 2022), conserve channel and riparian/ floodplain ecotones and help push the current Natural Flood Management agenda forward

(Lane, 2017). A possible solution is to undertake a Nationwide survey of headwater catchments, to identify the connectivity status of sediment cascades (Fryirs, 2017; Heckman et al., 2018) and thus determine their sensitivity status, hence signposting those that are most likely to respond to extreme events. This could adopt a combination of desk-based GIS-driven approaches to quantify connectivity (e.g. Heckman et al., 2018), and/or a modified version of the 'Fluvial Audit' (Sear and Newson, 2003), that more explicitly considers the factors raised in the discussion above. This paper has also demonstrated the potential role of morphodynamic modelling, in offering a tool to improve the river managers understanding of catchment- and reach-scale response to floods. The available resources are freely and widely available, not only the modelling software, but also in the form of multi-resolution DEMs (e.g. 1m-scale LiDAR), required to run the model. 'At-risk' headwater catchments could potentially be identified from national-scale ground-survey fluvial audits, which are then selected for more detailed morphodynamic modelling, in an attempt to understand possible future response to extreme floods.

Conclusions

An extreme summer flood in July 2007 resulted in activation of the sediment system and full valley-floor re-working for the 3rd order tributary of the Thinhope Burn, contrasting with the relatively stability shown in both neighbouring catchments. This study used morphodynamic modelling to demonstrate that Thinhope Burn is significantly more geomorphically effective to flood events than its neighbours, and demonstrated significantly greater geomorphic work (as quantified through sediment efflux) conducted by Thinhope, undertaken, both over the longer term (1998-2008), and during the July 2007 flood event. Reach-scale simulations demonstrated spatial patterns of adjustment (geomorphic work) in response to varying magnitude flows. Shear stress tended to increase with peak discharge and at around 60 m^3s^{-1} modal shear stresses peaked at around 450 Nm^{-2}. This suggested that flows in the region of 60 m^3s^{-1}, like that experienced in July 2007, may achieve 'peak' hydraulic output, and hence maximum geomorphic work. Thinhope Burn appeared to have a greater propensity for change and presently lacked an ability to recover, when compared to its neighbouring catchments.

Morphometric catchment attributes do not appear to offer an explanation for the differential response shown by Thinhope to the 2007 event. However it is argued that factors such as strength resistance of the key sediment sources (e.g. berms, lobes and splays perched on terraces) and the form resistance presented to flood waves passing through the narrow Thinhope valley may offer explanations for increased sensitivity. In addition two further sub-factors relating to sediment connectivity, namely; location sensitivity (juxtaposition of main sediment stores) and transmission resistance (ease to which morphological response is transmitted downstream) may further explanation the enhanced geomorphic effectiveness found in Thinhope Burn.

With the expectation of greater rainfall totals in the winter and more extreme events in upland areas of Britain, it is clear that attention needs to focus upon the possible implications of this on the morphological stability of these areas not least to aid future sustainable flood risk management. A combination of a modified fluvial audit approach (including desk-based GIS analyses of connectivity and field-based campaigns) and morphodynamic modelling may offer river managers a 'toolkit', that can provide valuable insight, into understanding catchments that present the greatest risk for future flooding. However, despite being nearly 20 years on from the introduction of the Fluvial Audit, it is clear that this has yet to be effectively rolled out and applied by river managers in Britain. Perhaps it is time to reflect on the advances made in fluvial geomorphology in the last two decades, and rethink upland river management to achieve flood risk, habitat and landform conservation objectives.

Acknowledgements

Thanks is extended to the British Society for Geomorphology for supporting the project through a research grant. Broader support for this long running project has also been provided by the Universities of Gloucestershire and Hull. Adam Watson is thanked for allowing us to access his land over the full duration of the study, as well as transporting us on his Quad Bike towards the head of Thinhope Burn, giving us access to otherwise inaccessible areas, whilst surveying the 2007 catchment wide flood impacts with the HYDRATE team. I am also grateful to Tom Coulthard who gave advice on parameterising early runs of the modelling and on selection of rainfall series, in the absence of an hourly long-term records close to the study site. This paper was written-up whilst David Milan was in receipt of an Institute of Advanced Study Fellowship at Collegium de Lyon.

References

Allan AF and Frostick LE (1999) Framework dilation, winnowing and matrix particle size: the behaviour of some sand–gravel mixtures in a laboratory flume. *Journal of Sedimentary Research* 69: 21–26.

Bain V, Gaume E and Bressy A (2010) Methods and case studies in post flood event data collection and analysis. Hydrometeorological Data Resources and Technologies for Effective Flash Flood Forecasting (HYDRATE), Deliverable Report 41, 43 pp.

Barinaga M (1996) A recipe for river recovery? *Science* 273:1648–1650.

Bartley R and Rutherfurd I (2005) Re-evaluation of the wave model as a tool for quantifying the geomorphic recovery potential of streams disturbed by sediment slugs. *Geomorphology* 64:221–242.

Bates PD and De Roo APJ (2000) A simple raster-based model for flood inundation simulation. *Journal of Hydrology* 236: 54-77.

Beniston M (2009) Trends in joint quantiles of temperature and precipitation in Europe since 1901 and projected for 2100. *Geophysical Research Letters* 36: L07707.

Beniston M Stoffel M and Hill M (2011) Impacts of climatic change on water and natural hazards in the Alps: Can current water governance cope with future challenges? Examples from the European ‘‘ACQWA’’ project. *Environmental Science & Policy* 14: 734-743.

Beven K (1981) The Effect of Ordering on the Geomorphic Effectiveness of Hydrologic Events, IAHS Publication 132. IAHS Press, Wallingford: 510–526.

Beven KJ and Kirkby MJ (1979) A physically based, variable contributing area model of basin hydrology / Un modèle à base physique de zone d’appel variable de l’hydrologie du bassin versant. *Hydrological Sciences Bulletin* 24: 43–69.

Borga M Anagnostou EN Blöschl G and Creutin JD (2011) Flash flood forecasting, warning and risk management: the HYDRATE project. *Environmental Science & Policy* 14: 834-844.

Bracken LJ Turnbull L Wainwright J and Bogaart P (2015) Sediment connectivity: a framework for understanding sediment transfer at multiple scales. *Earth Surface Processes and Landforms* 40: 177–188.

Bras RL Tucker GE and Teles V (2003) *Six myths about mathematical modeling in geomorphology*. Massachusetts Inst. of Tech, Cambridge Dept of Civil and Environmental Engineering.

Brayshaw AC (1985) Bed microtopography and entrainment thresholds in gravel-bed rivers. *Geological Society of America Bulletin* 96(2): 218-223.

Brierley G and Fryirs K (2009) Don't fight the site: three geomorphic considerations in catchment-scale river rehabilitation planning. *Environmental Management* 43: 1201-1218.

Brierley GJ and Fryirs KA (2005). *Geomorphology and River Management: Applications of the River Styles Framework*. Blackwell Publications: Oxford, pp. 398.

Brierley GJ and Fryirs KA (2016) The use of evolutionary trajectories to guide 'moving targets' in the management of river futures. *River Research and Applications* 32: 823-835.

Brunsden D (1990) Tablets of stone: toward the ten commandments of geomorphology. *Zeitschrift für Geomorphology* 79: 1–37.

Brunsden D (1993a) Barriers to geomorphological change. In: Thomas DSG and Allison RJ (eds) *Landscape Sensitivity*. Wiley, pp. 7–12.

Brunsden D (1993b) The persistence of landforms. *Zeitschrift für Geomorphology*. 93: 13–28.

Brunsden D (2001) A critical assessment of the sensitivity concept in geomorphology. *Catena* 42: 99-123.

Brunsden D and Thornes JB (1979) Landscape sensitivity and change. *Transactions of the Institute of British Geographers* 4: 463–484.

Carling PA (1983) Threshold of coarse sediment transport in broad and narrow natural streams. *Earth Surface Processes and Landforms* 8: 1-18.

Carling PA (1986) Peat slides in Teesdale and Weardale, Northern Pennines, July 1983: description and failure mechanisms. *Earth Surface Processes and Landforms 11*(2): 193-206.

Carling PA (1986) The Noon Hill flash floods; July 17th 1983. Hydrological and geomorphological aspects of a major formative event in an upland landscape. *Transactions of the Institute of British Geographers* 11: 105–118.

Carling PA (1987) Hydrodynamic interpretation of a boulder berm and associated debris-torrent deposits. *Geomorphology* 1(1): 53-67.

Carling PA (1989) Hydrodynamic models of boulder berm deposition. *Geomorphology 2*(4): 319-340.

Costa JE (1984) Physical geomorphology of debris flows. In *Developments and applications of geomorphology*, pp. 268-317)., Springer, Berlin, Heidelberg.

Costa JE 1988. Rheological, geomorphic and sedimentological differentiation of water floods, hyperconcentrated flows and debris flows. In Baker VR Kochel RC and Patton PC (Eds.) Flood Geomorphology, New York, John Wiley and Sons, pp113-122.

Costa JE and O'Connor JE (1995) Geomorphically effective floods. In: Costa JE Miller AJ Potter KW and Wilcock PR (eds) *Natural and Anthropogenic Influences in Fluvial Geomorphology*. American Geophysical Union, Washington, DC, pp. 45–56.

Coulthard TJ Lewin J and Macklin M (2005) Modelling differential catchment response to environmental change. *Geomorphology* 69: 222-241.

Coulthard TJ Neal JC Bates PD Ramirez J Almeida GAM and Hancock GR (2013) Integrating the LISFLOOD-FP 2D hydrodynamic model with the CAESAR model: Implications for modelling landscape evolution. *Earth Surface Processes and Landforms* 38: 1897–1906.

Dadson SJ Hall JW Murgatroyd A Acreman M Bates P Beven K Heathwaite L Holden J Holman IP Lane SN and O'Connell E (2017) A restatement of the natural science evidence concerning catchment-based ‘natural’ flood management in the UK. *Proceedings of the Royal Society A: Mathematical, Physical and Engineering Sciences*, 473: p.20160706.

Downs PW and Gregory KJ (1993) The sensitivity of river channels in the landscape system. In: Thomas DSG and Allison R (eds) *Landscape Sensitivity*. John Wiley & Sons, New York, pp. 15–30.

Downs PW and Gregory KJ (2004) *River Channel Management: Towards Sustainable Catchment Hydrosystems*. Arnold, London, pp. 395.

Dykes AP and Warburton J (2007) Mass movements in peat: a formal classification scheme. *Geomorphology* 86: 73-93.

Fryirs K (2013) (Dis) Connectivity in catchment sediment cascades: a fresh look at the sediment delivery problem. *Earth Surface Processes and Landforms* 38: 30-46.

Fryirs K and Brierley G (2000) A geomorphic approach to the identification of river recovery potential. *Physical Geography* 21: 244-277.

Fryirs KA (2017) River sensitivity: A lost foundation concept in fluvial geomorphology. *Earth Surface Processes and Landforms* 42: 55-70.

Fryirs KA and Brierley GJ (2016) Assessing the geomorphic recovery potential of rivers: forecasting future trajectories of adjustment for use in management. *Wiley Interdisciplinary Reviews: Water* 3: 727-748.

Gaume E Bain V Bernardara P Newinger O Barbuc M Bateman A Blaškovičová L Blöschl G Borga M Dumitrescu A and Daliakopoulos I (2009) A compilation of data on European flash floods. *Journal of Hydrology* 367: 10-78.

Gore JA (ed) (1985) The Restoration of Rivers and Streams: Theories and Experience. Boston, MA: Butterworth.

Graf WL (1979) Catastrophe theory as a model for change in fluvial systems. 10th Annual Geomorphology Symposium, Binghamton, New York.

Gregory KJ (ed) (1997) *Fluvial Geomorphology of Great Britain*. Springer Science & Business Media.

Groisman PY Knight RW Easterling DR Karl TR Hegerl GC Razuvaev VN (2005) Trends in intense precipitation in the climate record. *Journal of Climate* 18:1326–1350.

Groisman PY Knight RW Karl TR Easterling DR Sun B Lawrimore J (2004) Contemporary changes of the hydrological cycle over the contiguous United States: trends. *Journal of Hydrometeorology* 5: 64–85.

Gupta A and Fox H (1974) Effects of high-magnitude floods on channel form: a case study in Maryland Piedmont. *Water Resources Research* 10: 499–509.

Harvey AM (1986) Geomorphic effects of a 100 year storm in the Howgill Fells, Northwest England. *Zeitschrift für Geomorphologie* 30: 71-91.

Harvey AM (2001) Coupling between hillslopes and channels in upland fluvial systems: implications for landscape sensitivity, illustrated from the Howgill Fells, northwest England. *Catena* 42: 225–250.

Harvey AM (2007) Differential recovery from the effects of a 100-year storm: significance of long-term hillslope–channel coupling; Howgill Fells, northwest England. *Geomorphology* 84: 192–208.

Hassan MA and Reid I (1990) The influence of microform bed roughness elements on flow and sediment transport in gravel bed rivers. *Earth Surface Processes and Landforms* 15(8): 739-750.

Hauer FR Locke H Dreitz VJ Hebblewhite M Lowe WH Muhlfeld CC Nelson CR Proctor MF Rood SB (2016) Gravel-bed river floodplains are the ecological nexus of glaciated mountain landscapes. *Science Advances* 2: p.e1600026.

Haynes H and Pender G (2007) Stress history effects on graded bed stability. *Journal of Hydraulic Engineering* 33: 343–349.

Heckmann T Cavalli M Cerdan O Foerster S Javaux M Lode E Smetanová A Vericat D Brardinoni F (2018) Indices of sediment connectivity: opportunities, challenges and limitations. *Earth-Science Reviews* 187: 77-108.

Heritage G Entwistle N.S and Milan D (2019) Evidence of non-contiguous flood driven coarse sediment transfer and implications for sediment management. In: E-proceedings of the 38th IAHR World Congress. International Association for Hydro-Environment Engineering and Research.

Heritage GL Large ARG and Milan DJ (2022) *A Field Guide to British Rivers*. Wiley. ISBN 9781118487983

Hopkins J and Warburton J (2014) Local perception of infrequent, extreme upland flash flooding: prisoners of experience? *Disasters* 39: 546-569.

Huntington TG (2006) Evidence for intensification of the global water cycle: review and synthesis. *Journal of Hydrology* 319: 83–95.

Iseya F Ikeda H Maita H and Kodama Y 1992. Fluvial deposits in a torrential gravel-bed stream by extreme sediment supply: Sedimentary structure and depositional mechanism." In Billi P Hey R Tacconi P and Thorne CE (Eds.) Dynamics of Gravel-Bed Rivers, *John Wiley and Sons*.

Joyce HM Hardy RJ Warburton J and Large ARG (2018) Sediment continuity through the upland sediment cascade: geomorphic response of an upland river to an extreme flood event. *Geomorphology* 317: 45-61.

Kale VS Ely LL Enzel Y Baker VR (1994) Geomorphic and hydrologic aspects of monsoon floods on the Narmada and Tapi Rivers in central India. *Geomorphology* 10: 157–168.

Kendon EJ Roberts NM Fowler HJ Roberts MJ Chan SC and Senior CA 2014. Heavier summer downpours with climate change revealed by weather forecast resolution model. *Nature Climate Change*, 4(7):570-576.

Kleinen T and Petschel-Held G (2007) Integrated assessment of changes in flooding probabilities due to climate change. *Climate Change* 81: 283–312.

Kleinhans MG (2010) Sorting out river channel patterns. *Progress in Physical Geography* 34: 287-326.

Knox JC (1993) Large increases in flood magnitude in response to modest changes in climate. *Nature* 361: 430-432.

Knox JC (2000) Sensitivity of modern and Holocene floods to climate change. *Quaternary Science Reviews* 19: 439-457.

Kochel RC (1988) Geomorphic impact of large floods: review and new perspectives on magnitude and frequency. In: Baker K Kochel RC and Patton PC (eds). *Flood Geomorphology*, Wiley, Toronto, pp. 169–187.

Komar PD and Li Z (1986 Pivoting analyses of the selective entrainment of sediments by shape and size with application to gravel threshold. *Sedimentology* 33(3): 425-436.

Kondolf GM (1997) PROFILE: hungry water: effects of dams and gravel mining on river channels. *Environmental Management* 21: 533-551.

Lane SN (2017) Natural flood management. *Wiley Interdisciplinary Reviews: Water* 4: p.e1211.

Large ARG (1991) The Slievenakilla bog-burst: investigations into peat loss and recovery on an upland blanket bog. *The Irish Naturalists' Journal* 23: 354-359.

Leopold LB and Langbein WB (1962) *The concept of entropy in landscape evolution*. US Geological Survey Professional Paper 500-A: 20pp.

Lisenby PE Croke J Fryirs KA (2018) Geomorphic effectiveness: a linear concept in a non-linear world. *Earth Surface Processes and Landforms* 43: 4-20.

Macklin MG Rumsby BT and Heap T (1992) Flood alluviation and entrenchment: Holocene valley-floor development and transformation in the British uplands. *Geological Society of America Bulletin* 104: 631-643.

Magilligan FJ (1992) Thresholds and the spatial variability of flood power during extreme floods. *Geomorphology* 5: 373–390.

Manning R (1891) On the flow of water in open channels and pipes. *Transactions of the Institute of Civil Engineers, Ireland* 20: 61–207.

McCall I and Webb D 2016. Glenridding flood investigation report. Environment Agency and Cumbria County Council. https://www.cumbria.gov.uk/eLibrary/Content/Internet/536/6181/4255914426.pdf

Milan D and Schwendel A (2019) Long-term channel response to a major flood in an upland gravel-bed river. In: E-proceedings of the 38th IAHR World Congress, 2831-2838. IAHR.

Milan D Heritage G Tooth S and Entwistle N (2018) Morphodynamics of bedrock-influenced dryland rivers during extreme floods: Insights from the Kruger

National Park, South Africa. *Geological Society of America Bulletin* 130: 1825-1841.

Milan DJ (2012) Geomorphic impact and system recovery following an extreme flood in an upland stream: Thinhope Burn, northern England, UK. *Geomorphology* 138: 319-328.

Milan DJ and Schwendel A (2021). Climate-change driven increased flood magnitudes and frequency in the British uplands: geomorphologically informed scientific underpinning for upland flood-risk management. *Earth Surface Processes and Landforms*. DOI: 10.1002/esp.5206

Miles MJ and Kellerhals R (1981) Some engineering aspects of debris torrents. Can. Soc. Civ. Eng. 5th Can. Hydrotech. Conf., New Brunswick: 395-420.

Miles MJ and Kellerhals R 1981. May. Some engineering aspects of debris torrents. In *Proceedings, Fifth Canadian Hydrotechnical Conference, Fredericton, New Brunswick. The Canadian Society for Civil Engineering, Fredericton, New Brunswick, Canada*, pp. 395-420)

Milly PCD Betancourt J Falkenmark Hirsch RM Kundzewicz ZW Lettenmaier DP and Stouffer RJ (2008) Stationarity Is Dead: Whither Water Management? *Science* 319(1):573-574

Modrick TM and Georgakakos KP (2015) The character and causes of flash flood occurrence changes in mountainous small basins of Southern California under projected climatic change. *Journal of Hydrology: Regional Studies* 3: 12-336.

Napoli A Crespi A Ragone F Maugeri M and Pasquero C (2019) Variability of orographic enhancement of precipitation in the Alpine region. *Scientific Reports* 9: 1-8.

Newson MD (1980) The geomorphological effectiveness of floods – a contribution stimulated by two recent events in mid-Wales. *Earth Surface Processes* 5: 1–16.

Newson MD (1989) Flood effectiveness in river basins: progress in Britain in a decade of drought. In: *Floods, hydrological, sedimentological and geomorphological implications*. Workshop, joint meeting of the BGRG and the British Hydrological Society, pp. 151-169.

Nolan KM Lisle TE and Kelsey HM (1987) Bankfull discharge and sediment transport in northwestern California. In: *Erosion and Sedimentation in the Pacific Rim*, Corvallis Symposium. IHAS Press, Wallingford: pp. 439–449.

Ockelford AM and Haynes H (2013) The impact of stress history on bed structure. *Earth Surface Processes and Landforms* 38(7): 717-727.

Otto FE van der Wiel K van Oldenborgh GJ Philip S Kew SF Uhe P and Cullen H 2018. Climate change increases the probability of heavy rains in Northern England/Southern Scotland like those of storm Desmond—a real-time event attribution revisited. *Environmental Research Letters*, 13(2): p.024006.

Petit F (1994) Dimensionless critical shear stress evaluation from flume experiments using different gravel beds. *Earth Surface Processes and Landforms* 19(6): 565-576.

Phillips JD (2009) Changes, perturbations, and responses in geomorphic systems. *Progress in Physical Geography* 33: 17-30.

Phillips JD (2014) State transitions in geomorphic responses to environmental change. *Geomorphology* 204: 208-216.

Phillips, J.D. 1992. Nonlinear dynamical systems in geomorphology: revolution or evolution? *Geomorphology* 5: 219-229.

Pierson TC and Scott KM 1985. Downstream dilution of a lahar: transition from debris flow to hyperconcentrated streamflow. *Water resources research* 21(10): 1511-1524.

Pierson TC Costa JE and Vancouver W (1987) A rheologic classification of subaerial sediment-water flows. *Debris Flows/Avalanches: Process, Recognition, and Mitigation. Reviews in Engineering Geology. Geological Society of America* 7: 1-12.

Quesada-Román A and Villalobos-Chacón A (2020) Flash flood impacts of Hurricane Otto and hydrometeorological risk mapping in Costa Rica. *Geografisk Tidsskrift-Danish Journal of Geography* 120(2): 142-155.

Quesada-Román A Ballesteros-Cánovas JA Granados-Bolaños S Birkel C and Stoffel M (2020) Dendrogeomorphic reconstruction of floods in a dynamic tropical river. *Geomorphology* 359: 107133.

Reid I and Frostick LE (1984) Particle interaction and its effects on the thresholds of initial and final bedload motion in coarse alluvial channels. In Koster, EH and Steel RJS (Eds), Sedimentology of Gravels and Conglomerates. Canadian SOC. Petroleum Geologists Memoir, 10, 6168.

Reid I Frostick LE and Layman JT (1985) The incidence and nature of bedload transport during flood flows in coarse-grained alluvial channels. *Earth Surface Processes and Landforms* 10: 33–44.

Rickenmann D (1991) Bed load transport and hyperconcentrated flow at steep slopes. In: Armanini A and Di Silvio G (eds) *Fluvial Hydraulics of Mountain Regions*. Lecture Notes in Earth Sciences 37: 429-442.

Rodine JD and Johnson AM (1976) The ability of debris, heavily freighted with coarse clastic materials, to flow on gentle slopes. *Sedimentology* 23(2): 213-234.

Sayers PB Horritt M Carr S Kay A Mauz J Lamb R and Penning-Rowsell E 2020. Third UK Climate Change Risk Assessment (CCRA3): Future flood risk. *Research* *undertaken by Sayers and Partners for the Committee on Climate Change. Published by Committee on Climate Change, London*.

Schumm SA (1979) Geomorphic thresholds: the concept and its applications. *Transactions of the Institute of British Geographers New Series* 4: 485-515.

Schumm SA (1991) *To interpret the Earth: ten ways to be wrong*. Cambridge University Press, 144pp,

Schwendel AC and Milan DJ (2020) Terrestrial structure-from-motion: Spatial error analysis of roughness and morphology. *Geomorphology* 350: p.106883.

Scott KM 1988. Origins, behavior, and sedimentology of lahars and lahar-runout flows in the Toutle-Cowlitz River system, Mount St Helens, Washington. U.S. Geological Survey Professional Paper 422K, pp.1-22.

Sear DA and Newson MD (2003) Environmental change in river channels: a neglected element. Towards geomorphological typologies, standards and monitoring.*Science of the Total Environment* 310: 17-23.

Stoffel M Wyżga B and Marston RA (2016) Floods in mountain environments: A synthesis. *Geomorphology* 272: 1-9.

Thomas MF (2001) Landscape sensitivity in time and space— an introduction. *Catena* 42: 83–98.

Thompson C and Croke J (2013) Geomorphic effects, flood power, and channel competence of a catastrophic flood in confined and unconfined reaches of the upper Lockyer valley, southeast Queensland, Australia. *Geomorphology 197*: 156-169.

Van De Wiel MJ Coulthard TJ Macklin MG and Lewin J (2007) Embedding reach-scale fluvial dynamics within the CAESAR cellular automaton landscape evolution model. *Geomorphology* 90: 283-301.

Vischer D and Hager WH (1998) *Dam hydraulics* (Vol. 2). Chichester, UK: Wiley.

Walling DE (1983) The sediment delivery problem. *Journal of Hydrology* 65: 209-237.

Warburton J (2010) Sediment transfer in steep upland catchments (Northern England, UK): Landform and sediment source coupling. In: Otto JC and Dikau R (eds) *Landform-Structure, Evolution, Process Control*. Lecture Notes in Earth Sciences 115, 165-183.

Werner MGF Hunter NM and Bates PD (2005) Identifiability of distributed floodplain roughness values in flood extent estimation. *Journal of Hydrology* 314(1-4): 139-157.

Wilby RL Beven KJ and Reynard NS (2008) Climate change and fluvial flood risk in the UK: More of the same? *Hydrological Processes* 22: 2511-2523.

Wilcock PR and Crowe JC (2003) Surface-based transport model for mixed-size sediment. *Journal of Hydraulic Engineering* 129: 120-128.

Wohl E Barros A Brunsell N Chappell NA Coe M Giambelluca T Goldsmith S Harmon R Hendrickx JMH Juvik J McDonnell J and Ogden F (2012) The hydrology of the humid tropics. *Nature Climate Change* 2 (9): 655-662.

Wolman MG (1954) A method of sampling coarse river-bed material. *EOS, Transactions American Geophysical Union 35*(6): 951-956.

Wolman MG and Gerson R (1978) Relative scales of time and effectiveness of climate in watershed geomorphology. *Earth Surface Processes* and Landforms 3: 189-208.

Wolman MG and Miller JP (1960) Magnitude and frequency of forces in geomorphic processes. *Journal of Geology* 68: 54–74.

Wong JS Freer JE Bates PD Sear DA and Stephens EM (2015) Sensitivity of a hydraulic model to channel erosion uncertainty during extreme flooding. *Hydrological Processes 29*(2): 261-279.

Table 1 Defining fundamental geomorphic concepts

Geomorphic Concept	Definition	Related sources
Effectiveness	Ability of an event or combination of events to affect the shape or form of the landscape. May be quantified using a range of metrics the most widely accepted being 'effective discharge'; the flow that transports the most sediment over time. Sediment flux or measures of landscape morphological change may be used as measures of effectiveness.	Wolman and Miller, 1960; Wolman and Gerson 1978; Newson 1989; Lisenby *et al*., 2018
Sensitivity	The severity of a response to a disturbance relative to the magnitude of the disturbance force. Three important aspects; 1) Possibility of change; the ratio of impelling to resisting forces; where channel response occurs when transport forces overcome resisting forces, 2) Propensity for change; which reflects the proximity to intrinsic or extrinsic thresholds, and the 3) Ability to recover; defined as the ratio of recurrence interval to recovery time. Sensitive systems take longer to recover and hence have a longer recovery time in comparison to resilient systems, following a threshold-exceeding event.	Thornes, 1979; Schumm, 1991; Downs and Gregory, 1993; 2004; Phillips 2009; Brunsden and Thomas, 2001
Thresholds	Thresholds may either be classed as 'extrinsic', which characterises the response of a system to an external influence, often manifest by a change in landform e.g. from single-thread to braided, or 'intrinsic' whereby changes may occur without a change in the external variable. Examples of intrinsic thresholds in fluvial systems include the mobilisation of sediment grains, or those required to modify a morphological unit such as a bar, river bank, berm or terrace. The degree to which a system is 'sensitive' depends on the proximity of the system to an extrinsic threshold.	Schumm, 1979
Connectivity	Describes the efficiency of sediment supply and transfer through a river catchment. Stores are often (dis)connected from the sediment 'conveyor,' and their activation often requires more extreme events of a magnitude and duration capable of accessing the store and powerful enough to mobilise the grains and the 'form'.	Fryirs, 2013
Recovery	The trajectory of change toward an improved geomorphic condition. The role of connectivity in upland landscapes is identified as being a key control on recovery, due to the effects of sediment supply on channel morphology.	Harvey 2007; Brierley and Fryirs, 2009
Event sequencing	Magnitude, frequency and sequencing of rainfall events can play a significant role in determining the morphological response within a catchment. For example the high sediment transport rates shown in the headwaters of the Severn and Wye catchments during a 100-yr event in 1977, was thought to have been primed by a similar magnitude event earlier in 1973, which activated hillslopes, and improved sediment connectivity to the channel network.	Gupta and Fox, 1974; Beven, 1981; Nolan *et al*., 1987; Newson, 1980; Kochel 1988; Magilligan, 1992; Kale *et al*., 1994; Costa and O'Connor, 1995; Milan *et al*., 2018

Table 2 Morphometric characteristics of the study catchments. The grain-size information reported are for single reaches located in the vicinity of Knarburn: 54°51'34.48"N, 2°31'36.37"W; Thinhope Burn: 54°52'46.59"N, 2°31'15.70"W; Glendue Burn: 54°54'3.62"N, 2°31'6.30"W

Morphometric index	**Knar Burn**	**Thinhope Burn**	**Glendue Burn**
Catchment Area (*A*) (km^2)	17.20	11.00	4.80
Perimeter km	19.20	16.40	12.00
Total Stream length (km)	32.00	24.40	12.80
Drainage density	1.90	2.20	2.70
Shreve order	4.00	3.00	3.00
Catchment Length (*L*) (km)	3.50	3.00	2.13
Catchment width	2.38	1.25	1.13
Form Factor (*F*) $F = \frac{A}{L^2}$	1.40	1.22	1.06
Elongation ratio(*E*) $E = \frac{2\sqrt{\frac{A}{p}}}{L}$	0.24	0.36	0.76
Circularity ratio (*C*) $C = \frac{A}{L^2}$	0.59	0.51	0.42
Median Grain Size (m)	0.160	0.126	0.145
Bed slope	0.022	0.031	0.054

Table 3 Peak discharge estimations and approximate runoff rates for the study sites for the 17th July 2007 flood (adapted from Bain *et al.*, 2017).

Site	**Basin area (km^2)**	**Discharge (m^3s^{-1})**		**Specific Discharge (m^3s^{-1} km^2)**	**mm hr^{-1} equivalent**	**Radar max (mm hr^{-1})**	**Runoff coefficient**
		Max	85	7.7	27.82		
Thinhope Burn	11	Probable	60	5.5	19.64	30	0.65
		Min	50	4.5	16.36		
		Max	10	2.1	7.50		
Glendue Burn	4.8	Probable	6	1.3	4.50	17	0.03
		Min	6	1.3	4.40		
		Max	22	1.3	4.60		
Knar Burn	17.2	Probable	19	1.1	3.98	30	0.13
		Min	13	0.8	2.72		

Table 1 Defining fundamental geomorphic concepts

Geomorphic Concept	Definition	Related sources
Effectiveness	Ability of an event or combination of events to affect the shape or form of the landscape. May be quantified using a range of metrics the most widely accepted being 'effective discharge'; the flow that transports the most sediment over time. Sediment flux or measures of landscape morphological change may be used as measures of effectiveness.	Wolman and Miller, 1960; Wolman and Gerson 1978; Newson 1989; Lisenby *et al.*, 2018
Sensitivity	The severity of a response to a disturbance relative to the magnitude of the disturbance force. Three important aspects; 1) Possibility of change; the ratio of impelling to resisting forces; where channel response occurs when transport forces overcome resisting forces, 2) Propensity for change; which reflects the proximity to intrinsic or extrinsic thresholds, and the 3) Ability to recover; defined as the ratio of recurrence interval to recovery time. Sensitive systems take longer to recover and hence have a longer recovery time in comparison to resilient systems, following a threshold-exceeding event.	Thornes, 1979; Schumm, 1991; Downs and Gregory, 1993; 2004; Phillips 2009; Brunsden and Thomas, 2001
Thresholds	Thresholds may either be classed as 'extrinsic', which characterises the response of a system to an external influence, often manifest by a change in landform e.g. from single-thread to braided, or 'intrinsic' whereby changes may occur without a change in the external variable. Examples of intrinsic thresholds in fluvial systems include the mobilisation of sediment grains, or those required to modify a morphological unit such as a bar, river bank, berm or terrace. The degree to which a system is 'sensitive' depends on the proximity of the system to an extrinsic threshold.	Schumm, 1979
Connectivity	Describes the efficiency of sediment supply and transfer through a river catchment. Stores are often (dis)connected from the sediment 'conveyor,' and their activation often requires more extreme events of a magnitude and duration capable of accessing the store and powerful enough to mobilise the grains and the 'form'.	Fryirs, 2013
Recovery	The trajectory of change toward an improved geomorphic condition. The role of connectivity in upland landscapes is identified as being a key control on recovery, due to the effects of sediment supply on channel morphology.	Harvey 2007; Brierley and Fryirs, 2009
Event sequencing	Magnitude, frequency and sequencing of rainfall events can play a significant role in determining the morphological response within a catchment. For example the high sediment transport rates shown in the headwaters of the Severn and Wye catchments during a 100-yr event in 1977, was thought to have been primed by a similar magnitude event earlier in 1973, which activated hillslopes, and improved sediment connectivity to the channel network.	Gupta and Fox, 1974; Beven, 1981; Nolan *et al.*, 1987; Newson, 1980; Kochel 1988; Magilligan, 1992; Kale *et al.*, 1994; Costa and O'Connor, 1995; Milan *et al.*, 2018

Table 2 Morphometric characteristics of the study catchments. The grain-size information reported are for single reaches located in the vicinity of Knarburn: 54°51'34.48"N, 2°31'36.37"W; Thinhope Burn: 54°52'46.59"N, 2°31'15.70"W; Glendue Burn: 54°54'3.62"N, 2°31'6.30"W

Morphometric index	Knar Burn	Thinhope Burn	Glendue Burn
Catchment Area (*A*) (km^2)	17.20	11.00	4.80
Perimeter km	19.20	16.40	12.00
Total Stream length (km)	32.00	24.40	12.80
Drainage density	1.90	2.20	2.70
Shreve order	4.00	3.00	3.00
Catchment Length (*L*) (km)	3.50	3.00	2.13
Catchment width	2.38	1.25	1.13
Form Factor (*F*) $F = \frac{A}{L^2}$	1.40	1.22	1.06
Elongation ratio(*E*) $E = \frac{2\sqrt{\frac{A}{\pi}}}{L}$	0.24	0.36	0.76
Circularity ratio (*C*) $C = \frac{A}{L^2}$	0.59	0.51	0.42
Median Grain Size (m)	0.160	0.126	0.145
Bed slope	0.022	0.031	0.054

Table 3 Peak discharge estimations and approximate runoff rates for the study sites for the 17th July 2007 flood (adapted from Bain *et al.*, 2017).

Site	Basin area (km^2)	Discharge (m^3s^{-1})		Specific Discharge (m^3s^{-1} km^2)	mm hr^{-1} equivalent	Radar max (mm hr^{-1})	Runoff coefficient
		Max	85	7.7	27.82		
Thinhope Burn	11	Probable	60	5.5	19.64	30	0.65
		Min	50	4.5	16.36		
		Max	10	2.1	7.50		
Glendue Burn	4.8	Probable	6	1.3	4.50	17	0.03
		Min	6	1.3	4.40		
		Max	22	1.3	4.60		
Knar Burn	17.2	Probable	19	1.1	3.98	30	0.13
		Min	13	0.8	2.72		

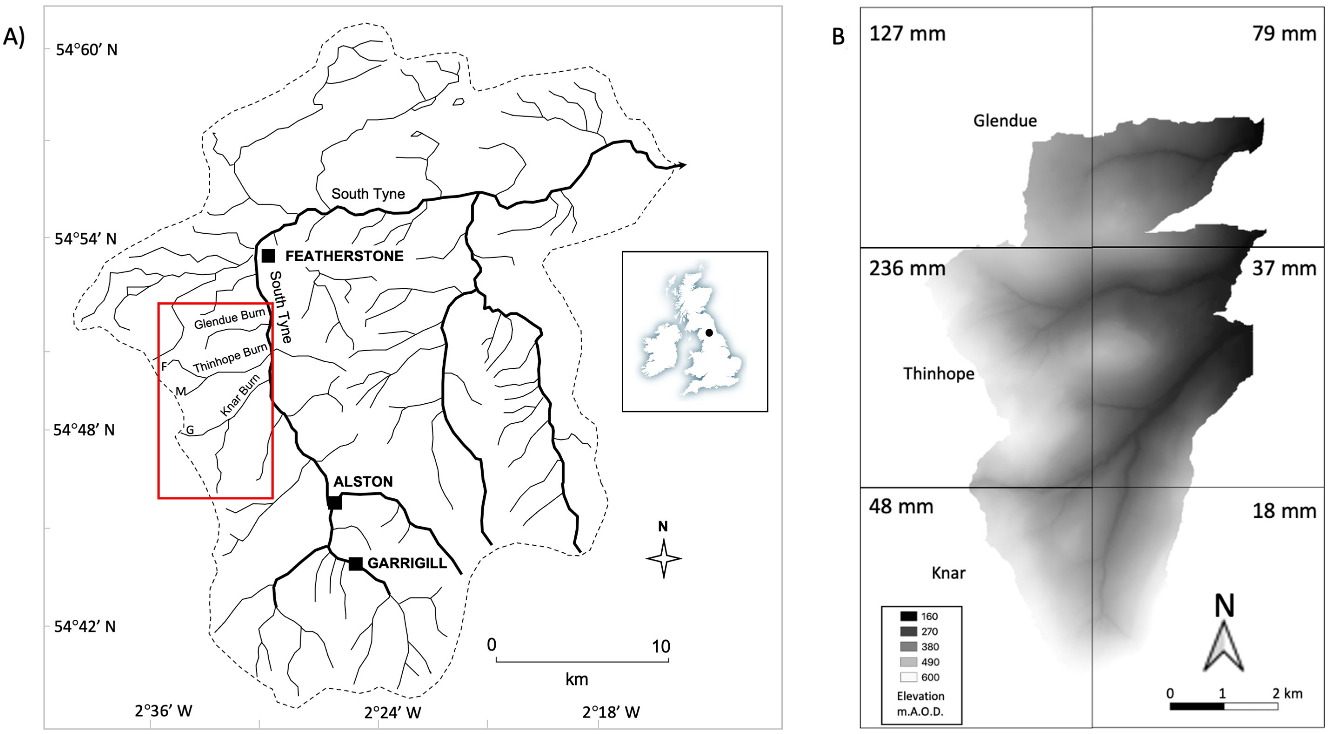

Figure 1 Study Catchments; A) South Tyne catchment and three sub-catchments at the centre of investigation. Tributaries to Thinhope Burn are indicated (M - Mardy's Cleugh; F – Feugh Cleugh), and Knar Burn (G – Gelt Burn); B) DEMs for neighbouring Knar, Thinhope and Glendue Burns. The 5km^2 NIMROD radar cells are overlain and the 24 hour rainfall totals are indicated in the corner of each cell.

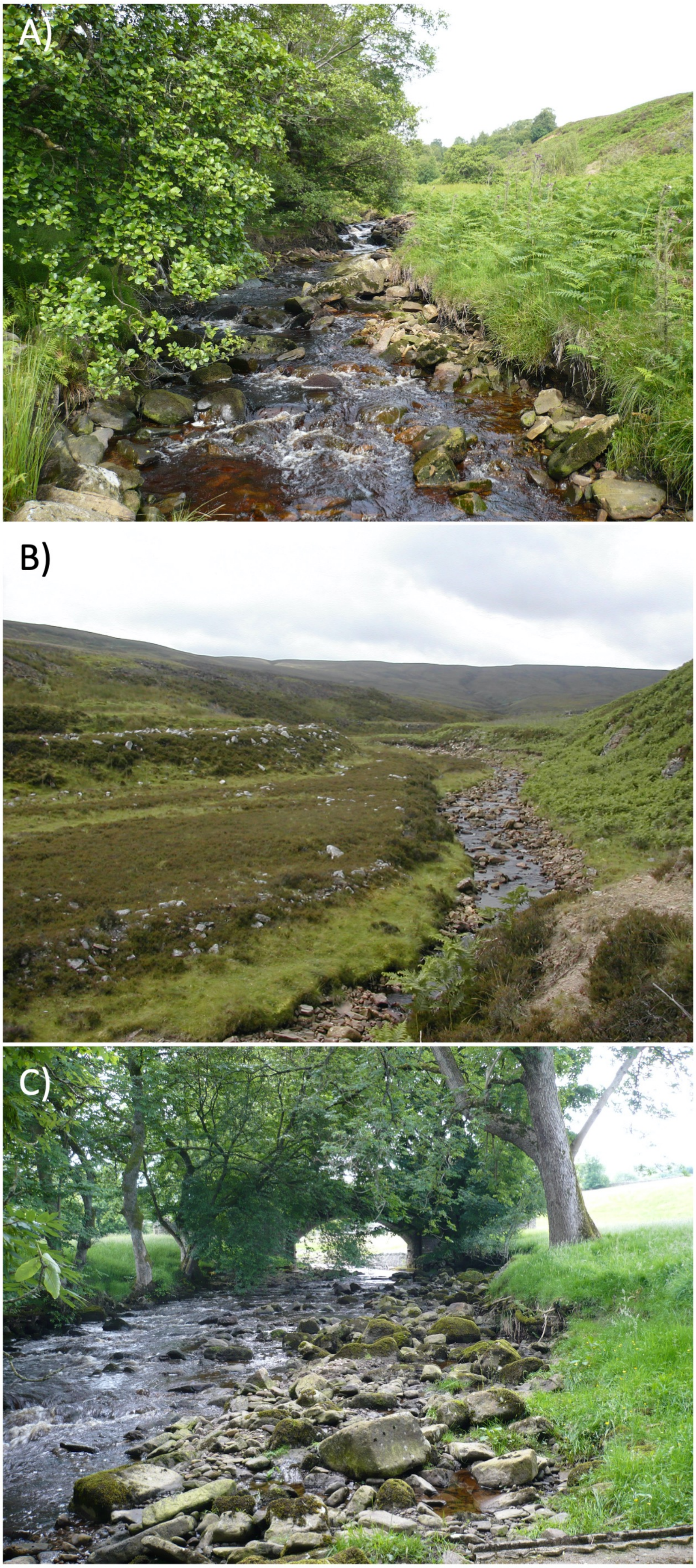

Figure 2 Photos of A) Glendue Burn (July 2008), B) Thinhope Burn (June 2004) and C) Knar Burn (July 2008)

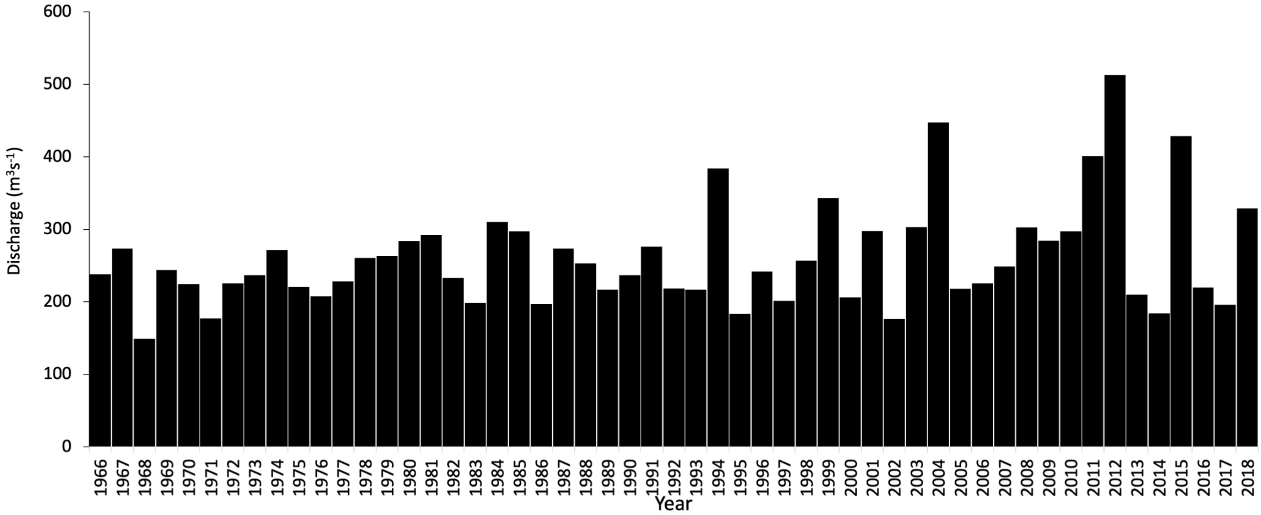

Figure 3 Annual peak flow data for the South Tyne and Featherstone, station 23006, (nrfa.ceh.ac.uk).

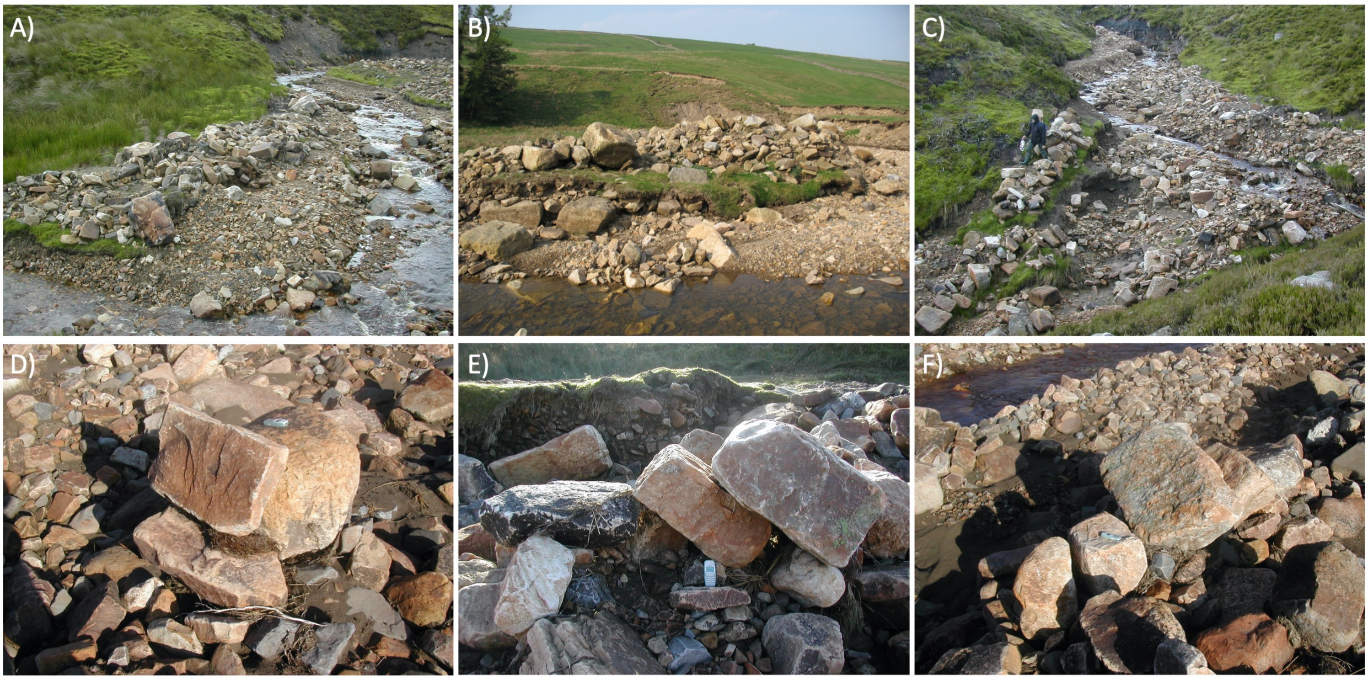

Figure 4. Morphological and sedimentological characteristics of deposits in the Thinhope Burn catchment, following the July 2007 flood event; A) and B) Berms deposited on the inside of meander bends on Thinhope Burn, C) Linear boulder ribbon deposited on floodplain in a steeper section of Mardy's Cleugh, D), E) and F) Boulder cluster bedforms; note the Nokkia 3410 mobile phone for scale.

Figure 5 The 500 m reach of Thinhope Burn where detailed morphological changes have been documented (see Milan, 2012; Milan and Schwendel, 2019; Schwendel and Milan, 2021), and use for reach-scale morphodynamic modelling in this paper (source: Google Earth Pro, 2021).

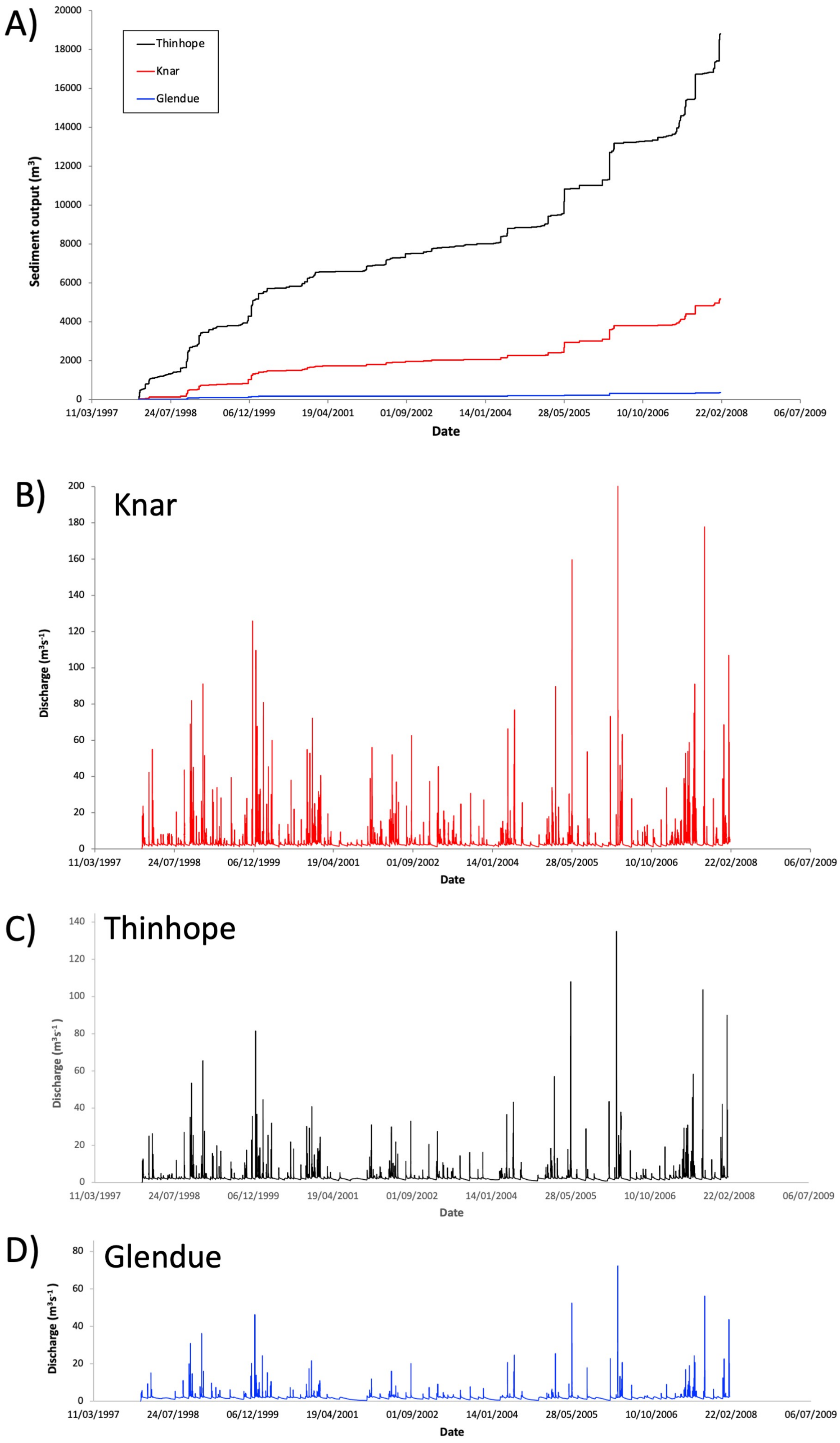

Figure 6 Time series plots showing A) cumulative sediment efflux from catchment scale runs for 1998-2007, simulated discharge for the B) Knar Burn, C) Thinhope Burn, D) Glendue Burn.

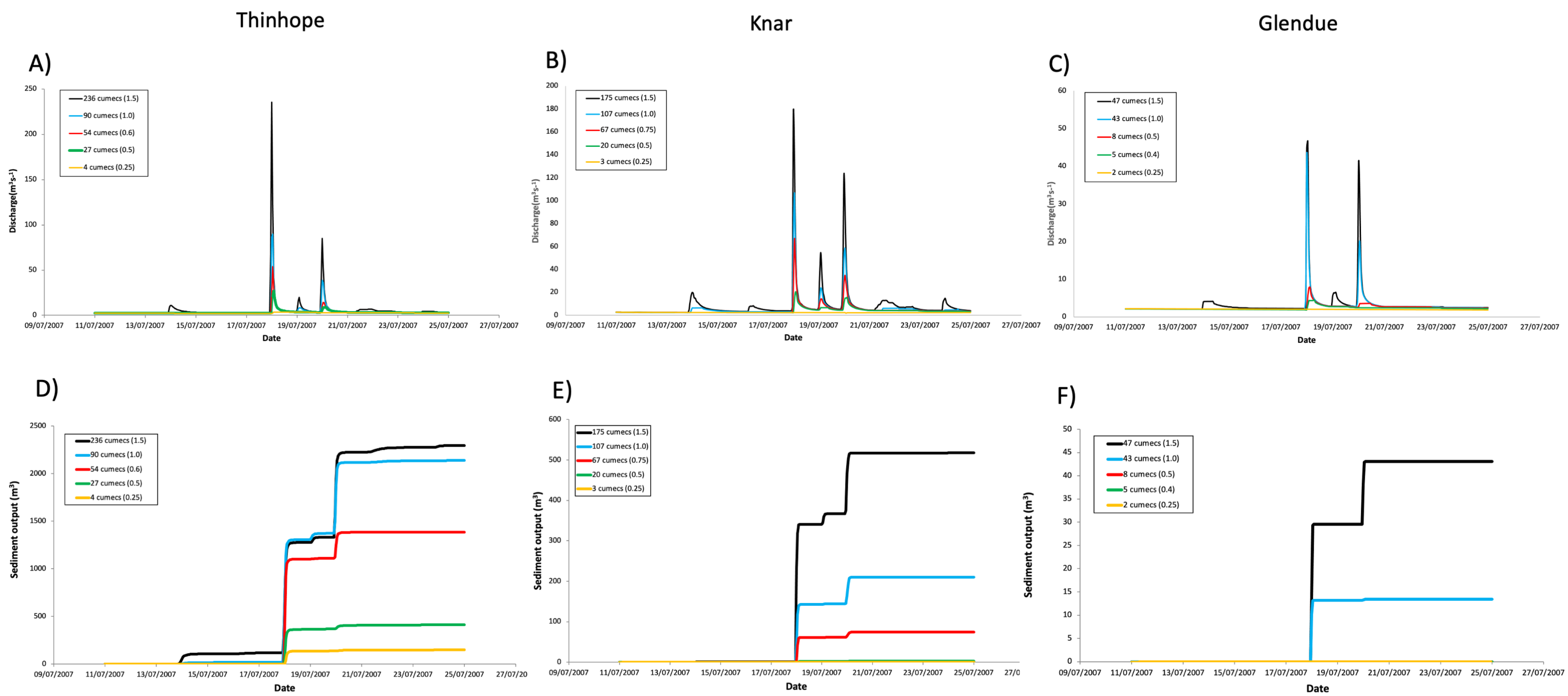

Figure 7 Results from CAESAR-Lisflood simulations over the14 day period between 11th-24th July 2007, following spin-up: A-C) Hydrographs produced using scaled rainfall inputs for the three study catchments, D-F) cumulative sediment efflux from the scaled model runs.

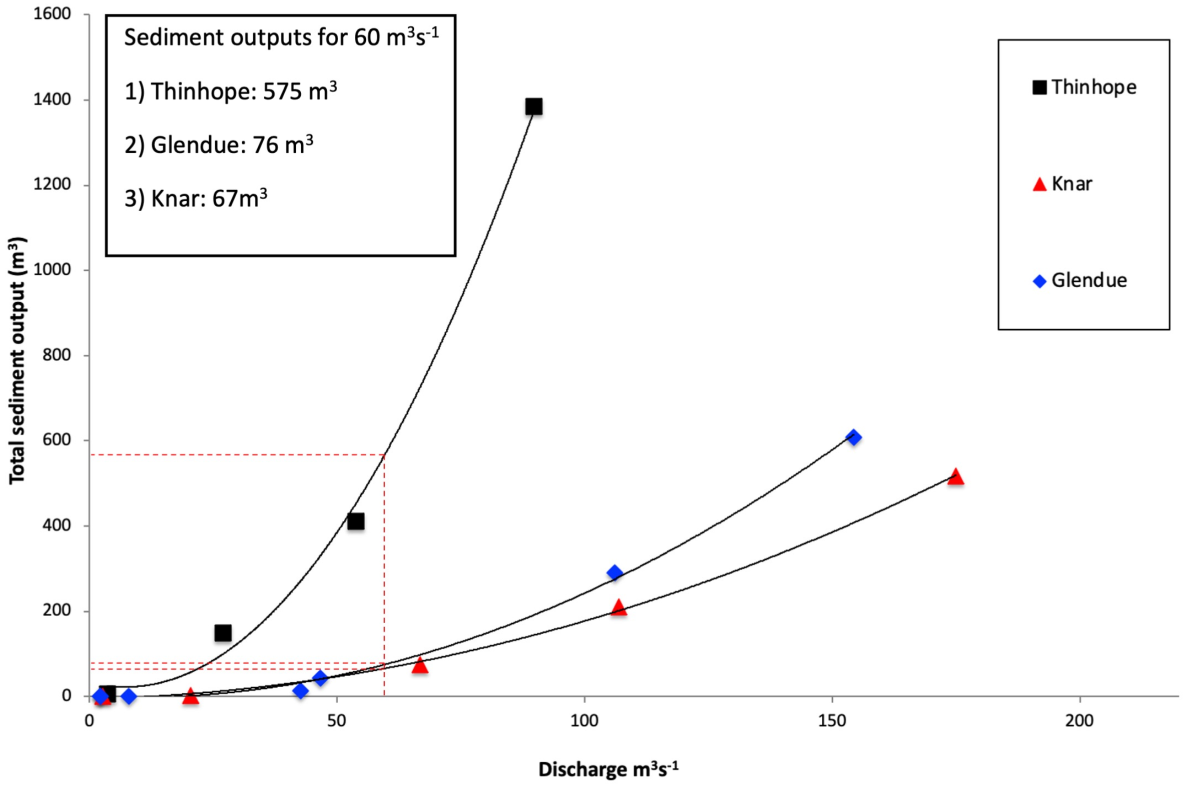

Figure 8 Total sediment efflux plotted against peak discharge for each scaled run, over the14 day period between 11th-24th July 2007, for the three study catchments.

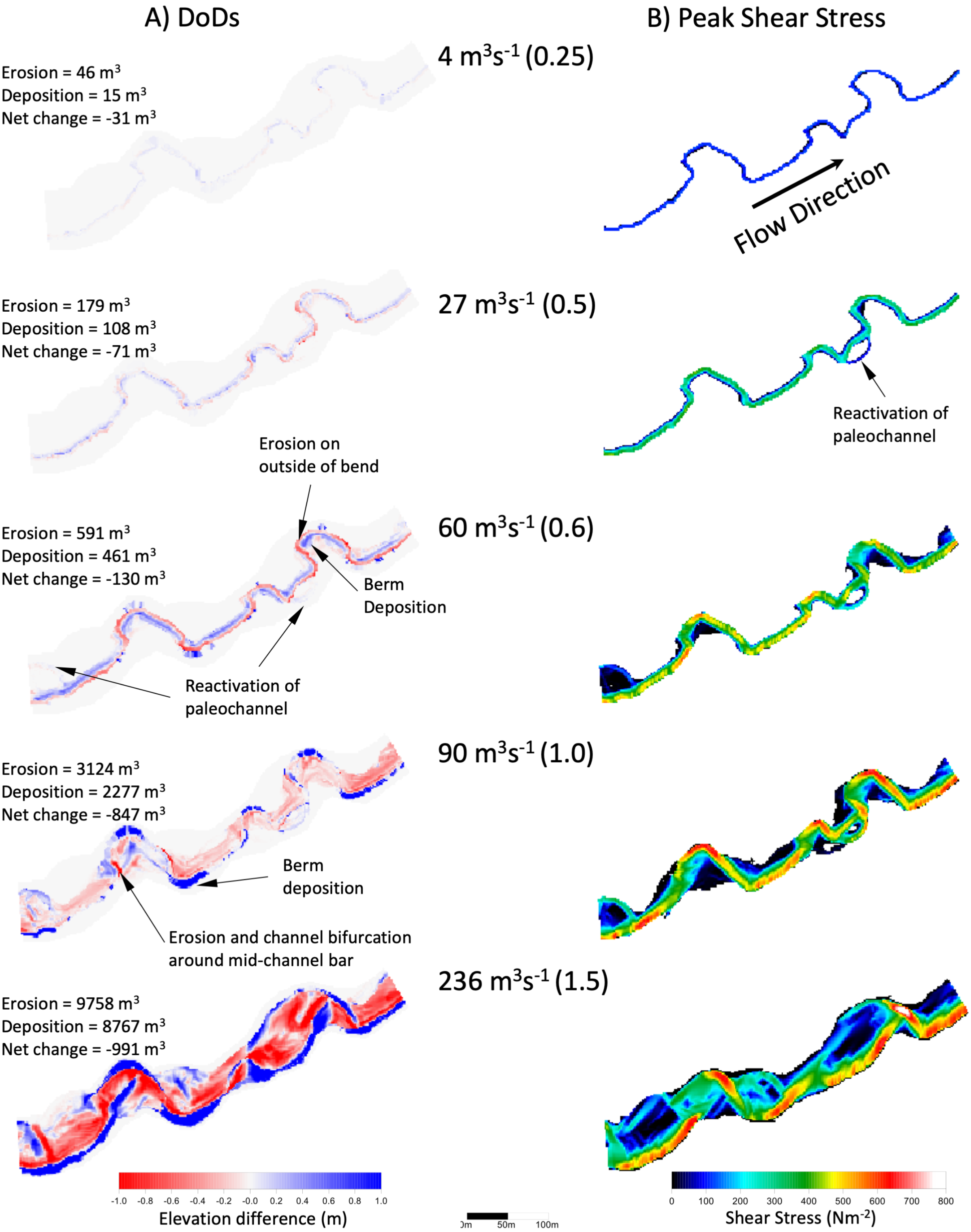

Figure 9 Reach-scale CAESAR-Lisflood output for Thinhope Burn: A) geomorphological work at the reach-scale using end-point rasters for DoD output for five of the different flow peaks generated from scaled rainfall data in the catchment-scale runs; B) shear stress rasters taken at each of the five flood peaks. N.B. Aerial photos showing actual response of the study reach to the 2007 event are shown in Figure 5.

Figure 10 Main sediment stores and sources on Thinhope Burn: A) pre-2007 flood boulder berm; B) eroding slope-channel coupling zones supplying till (base unit) and alluvium (near surface unit); C) tributaries; D) eroding terraces.

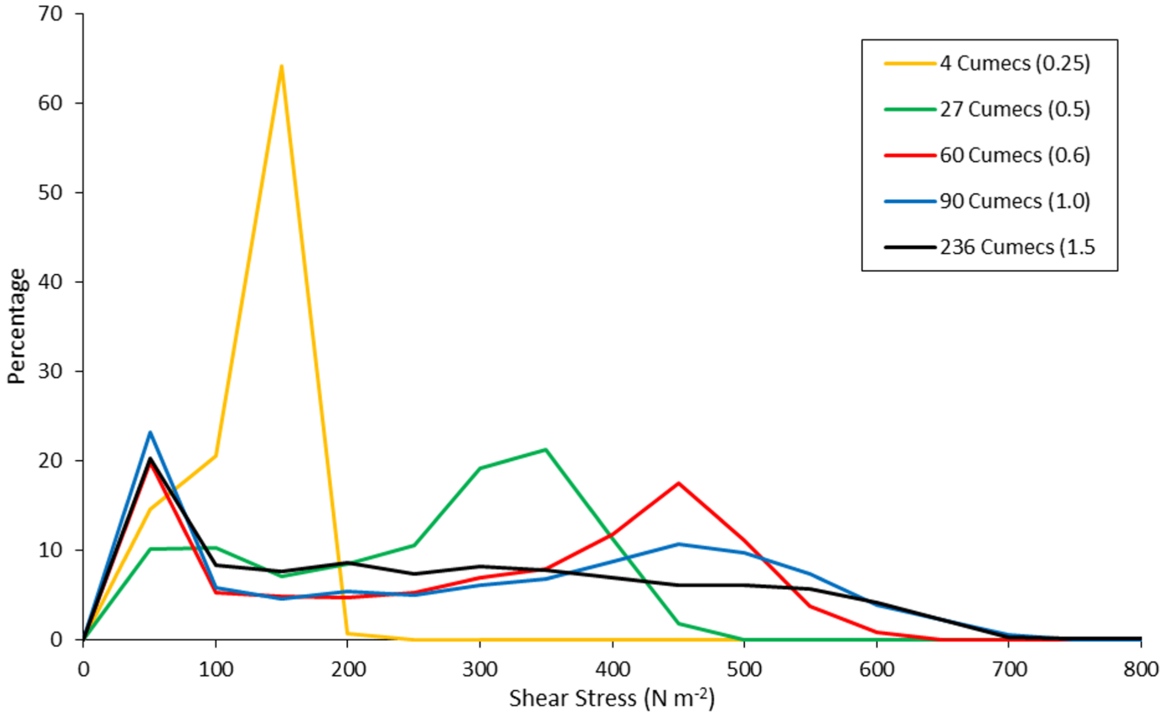

Figure 11 Population of shear stress for different flow peaks, using the values from each pixel from shear stress raster (Figure 9) generated using depth and velocity outputs from CAESAR-Lisflood outputs and through the application of Equation 1.